# POLITECNICO DI TORINO

**Master of Science**

**in Communication and Computer Network Engineering**

Master's Degree Thesis

# PROCESSING AND BEAMFORMING TECHNIQUES FOR CYLINDRICAL ARRAY IN 5G CELLULAR BASE STATIONS


**Academic Advisor:**

Supervisor: Prof. LADISLAU MATEKOVITS

Co-Supervisor: RIVIELLO DANIEL GAETANO

**Candidate:**

TAHA TARIQ (S260261)

**JULY-2021**

**Dedicated to my parents**

# Acknowledgement:

First of all, I would like to express my gratitude to Professor Ladislau Matekovits, for giving me the possibility to develop this thesis. I am thankful for his leadership, constant knowledge and experience sharing, as well as for his consistent availability, support, discipline, and professionalism even when there is horrible time of epidemic. Professor Ladislau was key during the production of this work, and important to my personal and academic advancement.

I also like to thank all my instructors, colleagues and friends that followed me along this journey from Politecnico Di Torino, specially giving their friendship, exchanging information, without forgetting the amusing moments. Without them, this path would be difficult.

Last, but not least, I owe to my parents and sister all my appreciation, to whom I dedicate my thesis, for their unconditional daily support, encouragement, belief, and for everything that they have done for me, as without them none of this would have been possible.

# ABSTRACT

The primary goal of antenna array design is to produce a radiation pattern determined by the antenna's amplitude and phase. Both features, amplitude, and phase, can be accomplished by adjusting factors such as the location of the feeding point, the patch's dimensions, the operating frequency, and the elements specified.

This thesis examines the 2-D conformal array antenna. A conformal antenna is one that is designed to take on any predetermined shape, in this case cylindrical. Cylindrical array antenna is the antenna in which we place numerous circular arrays vertically with specific radius. It is used in a variety of communication systems, navigation systems, and combat aircraft, among others.

Then, we began our discussion by presenting a quick overview of antennas and their many configurations, including linear, planar, and circular array antennas, as well as how they aid with 5G technology.

With the evolutions in the field of wireless communication have a significant impact not only on the environment but also on our daily life. In this research work a technique called beam scanning is introduced. To observe the performance of the conformal antenna on 2.45 GHz frequency, and to find the best results using these designs, Microwave Studio by CST is used for simulation purposes.

Firstly, the initial design of the conformal antenna is created with the single patch. The simulation is conducted on these single patches one by one, and the resulting simulation pattern are studied. With the help of these results, the successful dimensions of the patches on 2,45GHz were obtained as well as with the discrete port position of each patch.

The conformal antenna design incorporates sixteen elements arranged in a circle with four circles stacked on top of one another. On one side of the cylinder's substrate surface are antenna patches, with a copper ground plane on the opposite end.

Element patches are attached to ground plane through discrete ports crossing through substrate material. Each of the 64 patches is supplied independently by a discrete port. Rogers RT5880 substrate and copper ground (annealed) are employed in the design.

This thesis also includes theoretical analysis and, using the CST microwave studio software, simulation study with graphical representation for beam scanning.

The experimental results obtained show a good agreement with numerical simulation and therefore revalidate the approach used. This concept can be extended to base stations with the necessary adjustment of the radius of the supporting cylinder.

**Index Terms** –antenna array, beamforming, beam scanning, gain, efficiency, linear array antenna, planar array antenna, circular array antenna, cylindrical array antenna, conformal antenna

# Table of contents

**Acknowledgement:** ..... 3

**ABSTRACT** ..... 4

**List of Figures** ..... 9

**List of Tables** ..... 13

**Chapter 1: Introduction** ..... 14

*1.1 Brief Overview of Antenna* ..... 14

*1.2 Antennas and Modern Technology:* ..... 15

*1.3 Thesis Contribution* ..... 15

*1.4 Outline of Thesis:* ..... 16

**Chapter 2: Review of Literature** ..... 17

*Antenna array principles and classifications* ..... 17

*2.1 Antenna Parameters:* ..... 17

*2.1.1 Antenna Radiation Pattern:* ..... 18

*2.1.2 Antenna Directivity:* ..... 21

*2.1.3 Antenna gain:* ..... 23

*2.1.4 Antenna efficiency:* ..... 25

*2.1.5 Polarization:* ..... 26

*2.1.5 Bandwidth:* ..... 27

*2.1.6 Input Impedance:* ..... 27

*2.2 Antenna Beamforming:* ..... *29*

*2.2.1 Principles of Beamforming:* ..... 30

*2.2.2 Beam Steering and Beam Switching:* ..... 32

*2.2.3 Beamforming for Capacity and Coverage:* ..... 33

*2.3 Types of Antenna array:* ..... *34*

*2.3.1 Linear Array Antenna:* ..... 34

*2.3.2 Planar Array Antenna:* ..... 36

*2.3.3 Circular Array Antenna:* ..... 40

*2.3.4 Cylindrical Array Antenna:* ..... 43

*2.3.5 Conformal Array Antenna:* ..... 45

**Chapter 3: Design and Simulation ..... 48**

*3.1 Simulation tool:* ..... *48*

*3.2 Cylindrical Conformal Array:* ..... *48*

*3.3 Design of conformal array antenna:* ..... *48*

*3.3.1 Rogers RT5880 substrate:* ..... 51

*3.4 Simulation Setup and Results:* ..... *52*

*3.4.1 When having same Amplitude and Phase shift:* ..... 65

*3.4.2 When having same Amplitude but positive Phase shift:* ..... 67

*3.4.3 When having same Amplitude and negative Phase shift:* ..... 69

*3.4.4 When having different amplitude and positive Phase shift:* ..... 71

*3.4.5 When having different amplitude and negative Phase shift:* ..... 73

**Chapter 4: Conclusion ..... 75**

**Bibliography ..... 77**

# List of Figures

Figure 1 2.1: Array of equally distance elements [2] ..... 17

Figure 2 2.1.1 (a): Radiation pattern representation in coordinate system [3] ..... 18

Figure 3 2.1.1 (b): Lobe's representation of an antenna [3] ..... 19

Figure 4 2.1.1 (c): Fields's representation of an antenna [3] ..... 21

Figure 5 2.1.2: Isotropic antenna pattern [5] ..... 23

Figure 6 2.1.4 Antenna's reference terminals, losses, reflection, and conduction [3] ..... 25

Figure 7 2.1.5: Polarization of an antenna [7] ..... 26

Figure 8 2.1.6 Examples of different transmitting antennas [3] ..... 28

Figure 9 2.2: Beamforming schematic Diagram [3] ..... 29

Figure 10 2.2.1.1: Single and double antenna radiating pattern [5] ..... 30

Figure 11 2.2.1.2: Two and four elements radiating pattern [5] ..... 31

Figure 12 2.2.2.1: Beam steering and beam switching [7] ..... 32

Figure 13 2.2.2.2: Radiating patterns of common frequency and differing frequencies [5] ..... 33

Figure 14 2.2.3: Beamforming for capacity and coverage [3] ..... 33

Figure 15 2.3.1: Linear array of M-elements [3] ..... 34

Figure 16 2.3.1 Multiplication pattern of array factor, element, and total of 2-D array [3] ..... 35

Figure 17 2.3.2.1: Planar array of MxN elements [3] ..... 37

Figure 18 2.3.2: 3-D representation of planar array radiation pattern [8] ..... 38

Figure 19 2.3.3.1: N elements Circular array antenna [3] ..... 40
Figure 20 2.3.3.2: 3-D representation of circular array radiating pattern [8]..... 41
Figure 21 2.3.4.1: NxM element cylindrical array antenna [3] ..... 43
Figure 22 2.3.4.2: 3-D representation of 32x4 elements cylindrical array radiating pattern [8] ..... 45
Figure 23 2.3.5.1: Conformal cylindrical antenna [16]..... 46
Figure 24 2.3.5.2: Conformal antenna for aircraft wing integration [16] ..... 46
Figure 25 3.3: Conformal antenna of 4x16 configuration ..... 49
Figure 26 3.3: Equally spaced elements ..... 49
Figure 27 3.3: Single element dimension [3]..... 50
Figure 28 3.3.1: Dielectric loss versus frequency for different types of dielectric substrate materials [22] ..... 51
Figure 29 3.3.2: Discrete port of single element ..... 52
Figure 30 3.3.2: S-parameter with initial port location ..... 53
Figure 31 3.3.2: Repositioned Discrete port location ..... 53
Figure 32 3.3.2: S-parameter with repositioned port location ..... 54
Figure 33 3.3.2: Optimizer window in CST ..... 55
Figure 34 3.3.2: Resulting S-parameter after optimization..... 55
Figure 35 3.3.2: Discrete Ports using transform function ..... 56
Figure 36 3.3.2: Field Monitor window in CST ..... 56
Figure 37 3.3.2: Polar coordinates representation for equal Amplitude and Phase in XY plane ..... 57

Figure 38 3.3.2: Polar coordinates representation for equal Amplitude and Phase in XZ plane ..... 57
Figure 39 3.3.2: 3-D representation for equal Amplitude and Phase ..... 58
Figure 40 3.3.2: Conformal antenna of 4x5 configuration ..... 59
Figure 41 3.3.2: Discrete ports on center column ..... 59
Figure 42 3.3.2: S-parameter result of port 12 ..... 60
Figure 43 3.3.2: Polar coordinates representation of equal amplitude and phase of port 12 ..... 60
Figure 44 3.3.2: S-parameter result of port 13 ..... 61
Figure 45 3.3.2: Polar coordinates representation of equal amplitude and phase of port 13 ..... 61
Figure 46 3.3.2: S-parameter result of port 14 ..... 62
Figure 47 3.3.2: Polar coordinates representation of equal amplitude and phase of port 14 ..... 62
Figure 48 3.3.2: S-parameter result of port 15 ..... 63
Figure 49 3.3.2: Polar coordinates representation of equal amplitude and phase of port 15 ..... 63
Figure 50 3.4: 3-D representation of Farfield with same amplitude and phase shift .. 65
Figure 51 3.4: Polar coordinate representation of same amplitude and phase shift .. 66
Figure 52 3.4: 3-D representation of Farfield with same amplitude and positive phase shift ..... 67
Figure 53 3.4: Polar coordinate representation of same amplitude and positive phase shift ..... 68

Figure 54 3.4: 3-D representation of Farfield with same amplitude and negative phase shift ..... 69
Figure 55 3.4: Polar coordinate representation of same amplitude and negative phase shift ..... 70
Figure 56 3.4: 3-D representation of Farfield with different amplitude and positive phase shift ..... 71
Figure 57 3.4: Polar coordinate representation of different amplitude and positive phase shift ..... 72
Figure 58 3.4: 3-D representation of Farfield with different amplitude and negative phase shift ..... 73
Figure 59 3.4: Polar coordinate representation of different amplitude and negative phase shift ..... 74

# List of Tables

Table 1 Table of conformal design dimensions in millimeter ..... 50

Table 2 Post processing parameters of same amplitude and Phase shift ..... 65

Table 3 Post processing parameters of same amplitude and different Phase shift ..... 67

Table 4 Post processing parameters of same amplitude and negative Phase shift ..... 69

Table 5 Post processing parameters of both different amplitude and Phase shift ..... 71

Table 6 Post processing parameters of different amplitude and negative Phase shift .. 73

# Chapter 1: Introduction

## *1.1 Brief Overview of Antenna*

With the increasing growth of mobile data and communication over the last decade, there was a need for commercial as well as private users for a higher data, more stable connection, which resulted in the development of 4th generation technology and already 5th generation technology. However, in order to accomplish these greater performance levels, more complex equipment was required, one of which is a wireless antenna. An antenna is a device that takes an electromagnetic signal and converts it to an electric signal, or that changes an electric signal into an electromagnetic signal and radiates it.

It is primarily utilized as a communication medium, with various types of antennas supporting a variety of applications. It is a necessary component of wireless communication, from the antennas embedded in mobile phones through the telecommunications infrastructure. Other fields where antennas are used include surveillance, television transmission, and radar technology, to name a few.

As technology advances, a need for more advanced and better configured antennas arises, and thus the development of antenna arrays commences. An array of antennas is a configuration in which numerous antennas are connected and work in conjunction to provide the desired output.

Depending on the architectural design we select, every element of the array can indeed be fed separately or via a single feed. Each array of antennas is unique in terms of its specifications, which include the dimensions of the patches, the spacing between patches, the operating frequencies, the substrate material used, the thickness of the material used, and the placement of the feed. With array antennas, the user can create specific radiation patterns and steer them in the desired directions. Numerous research projects have been conducted on these types of antenna designs, and more will be conducted in the future to pave the way for even more advanced and improved technology utilization by users.

## 1.2 Antennas and Modern Technology:

The fast advancement of wireless communication technology implies a need for increasingly sophisticated solutions, which involve the transmission of data. The antenna is a critical component of that transmission. Matching the required strength and radiation pattern over long distances is quite difficult with a conventional single antenna. As a result, an antenna array solution is offered. Which enables higher gains, a narrower beam, and improved radiation patterns over extended distances.

These antenna arrays are more popular in today's 4G and 5G networks. Additionally, they should have a high gain to compensate for the significant path loss at mm-wave frequencies in 5G networks. Another type of antenna, the microstrip patch antenna, was developed to meet these objectives, although it too had limitations in terms of bandwidth and radiation efficiency.

As a result, many antenna designs are proposed to achieve the desired outcomes of the 5G network. A technology called beamforming is utilized in 5G networks to achieve a better directional gain and a narrow beam. Beamforming is accomplished by employing an array antenna element and altering the phase of these elements to generate a powerful directional beam directed in intended direction. The main lobe is formed between the two nulls along either side of the beam pointing direction. The width of the beam (primary lobe) between two half-power points is referred to as the half-power beamwidth, while other minor side radiations are referred to as sidelobes, which are typically undesirable since they radiate signal in an undesirable direction.

## 1.3 Thesis Contribution

The main contribution of the study is the combination of theoretical and simulation of the techniques used such as the calculations of the cylinder radius, patch elements dimensions, discrete port positioning, and substrate material. Another contribution lies in the experience gained through the process of designing the cylindrical conformal antenna

and an interpretive approach and optimization techniques applied for obtaining desired simulation results.

The practical contribution of this thesis work is the detailed insight study from the simulation results for different cases used for antenna designing. The simulation results revealed that how the dimensions of a single antenna patch can affect operating frequency as well as bandwidth of the antenna. It can also be seen that different theoretical values are used to obtain an optimal antenna design with the operating frequency of 2.45GHz. The contribution of this research is to understand, with the help of theoretical calculations, how an optimal cylindrical antenna is designed and used to perform beam scanning techniques.

## *1.4 Outline of Thesis:*

In this thesis cylindrical design of conformal antenna is observed by conducting theoretical investigation, implementation of codes, creation of antenna and its patches design with the use of commercially available simulation tool and the analysis of the results obtained.

The thesis is structured as follows: In Chapter 1, a brief review of the antenna and its application in current technology is addressed, along with an introduction to the beamforming process. Chapter 2 examines antenna parameters, beamforming techniques, and various antenna array configurations. Chapter 3 outlines the designs and simulations created for the thesis using CST software. Additionally, it discusses in depth the results gained from structural designs, the resulting graphs, the optimization results, and the graphs obtained from simulation results. Finally, Chapter 4 concludes.

# Chapter 2: Review of Literature

## *Antenna array principles and classifications*

Antenna arrays are frequently utilized to optimize the system's overall performance. They continue to be at the heart of mobile communication's present and future growth. The term "antenna array" refers to a collection of elements that are separated by a specific inter-element spacing. By arranging these elements, we can control the array's gain, radiation patterns, and directivity[1]. The gain of an antenna increases as radiation density in a particular direction increases[1].

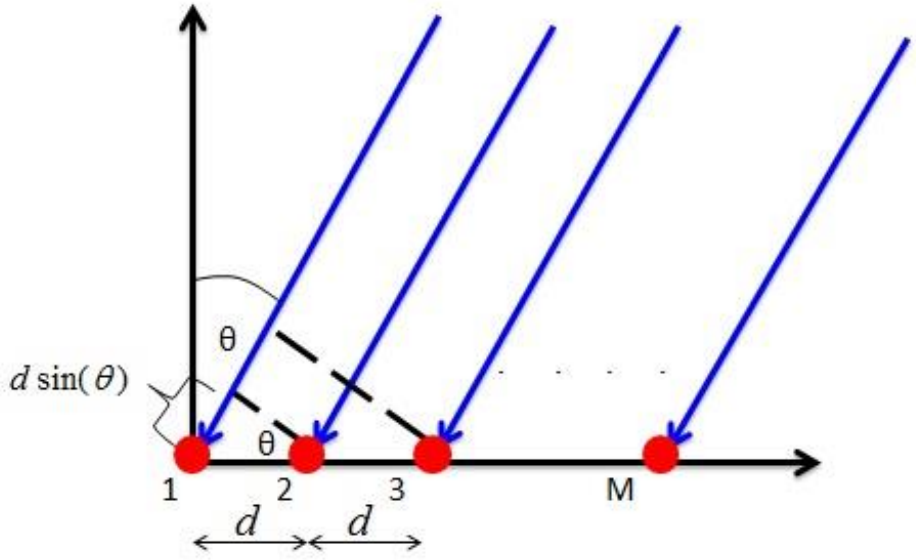


**Figure 1 2.1: Array of equally distance elements [2]**

When d=λ/2, which is inter-element spacing, and the array factor for isotropic M-elements is calculated by[2]

$$AF = 1 + e^{j(kd\cos\theta+\beta)} + e^{j2(kd\cos\theta+\beta)} + \ldots + e^{j(N-1)(kd\cos\theta+\beta)}$$

## *2.1 Antenna Parameters:*

An antenna's performance is highly dependent on a number of critical parameters. The gain of the antenna, the efficiency of the antenna, the radiation characteristics, the

bandwidth, the polarization, and the directivity of the antenna are just a few of the critical aspects to consider.

### *2.1.1 Antenna Radiation Pattern:*

The radiation pattern of an antenna can be conceived of as a graphical representation of the antenna's radiation qualities in a coordinate system. Such radiation patterns may be observed with an angular distribution in far field region [3]. These radiation patterns are critical for antenna representation because they represent critical factors like as directivity, radiation intensity, phases, gains, field strength, power flux density, and polarization[3].

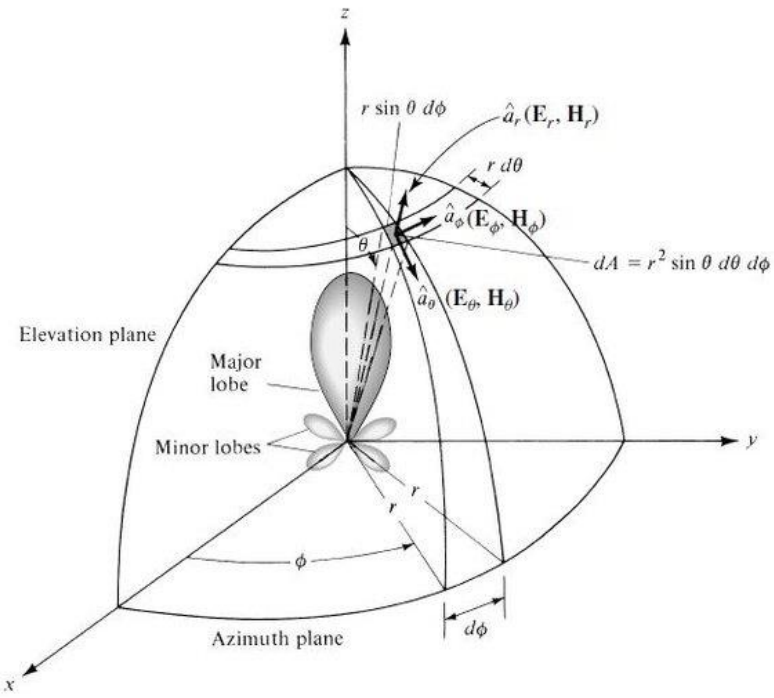


**Figure 2 2.1.1 (a): Radiation pattern representation in coordinate system [3]**

Furthermore, the above illustration introduces the concept of the major lobe, or direction of highest radiation. We have back lobe at phase shifts 180 degrees of main lobe. Along with the major lobe, side lobes are present[3].

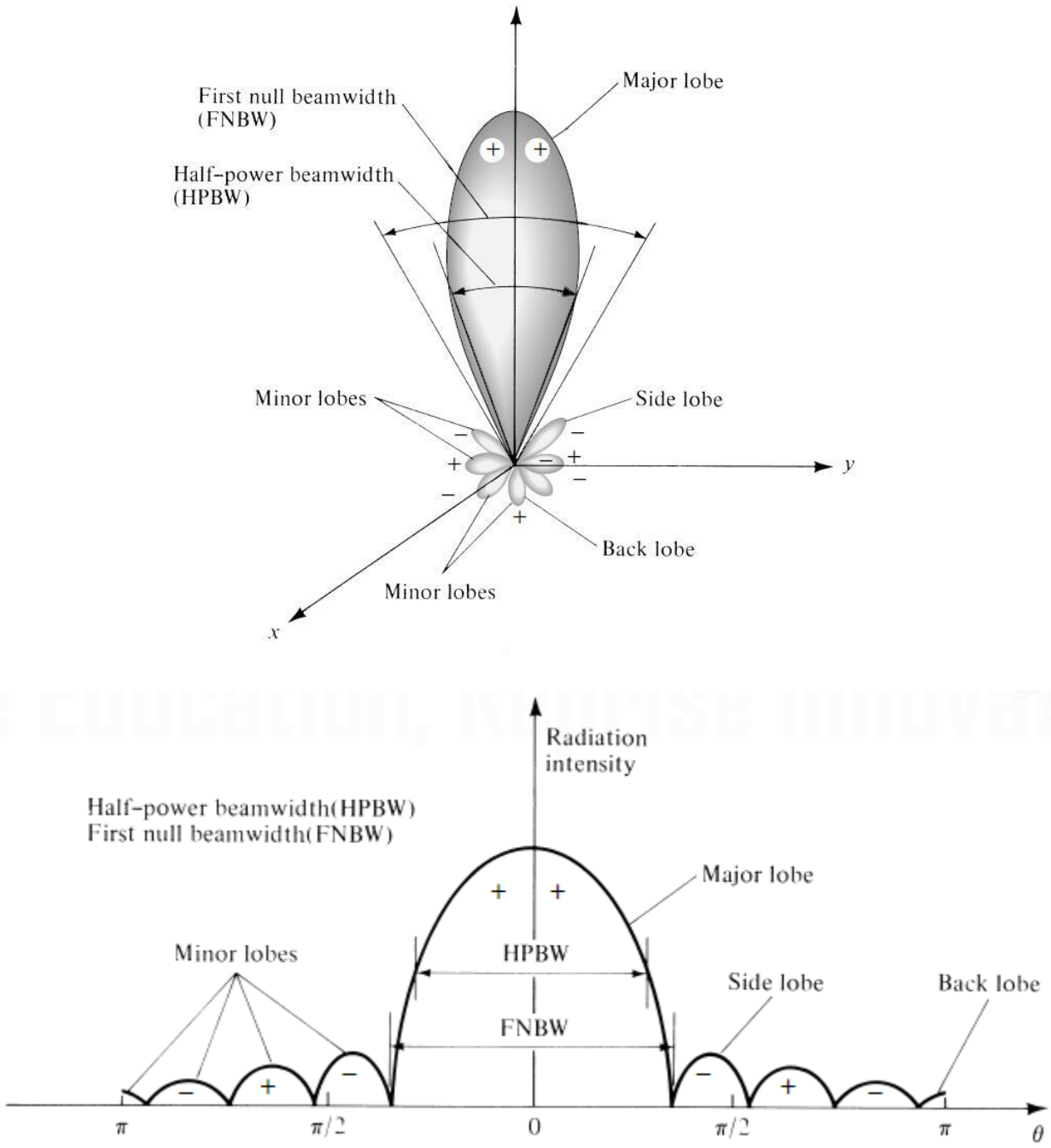


**Figure 3 2.1.1 (b): Lobe's representation of an antenna [3]**

Two critical parameters are depicted in the image above. To begin, first null beamwidth (FNBW) is the angle between the major lobe's initial nulls, whilst half power beamwidth (HFBW) is an angle on the major lobe where the signal strength is half of the overall peak value[4]. Beam topic is further discussed in beamforming section.

When an antenna transmits an electromagnetic wave, it divides into two distinct regions: the near field and the far field. Near field region refers to the region created nearby to an antenna [5].

$$Near\ Field\ Region < \frac{2D^2}{\lambda}$$

Where D = Maximum linear dimension of the antenna

$\lambda$ = Wavelength of the EM Waves

The near field region is further subdivided into reactive near field and radiative near field. The reactive near field region is the area adjacent to the antenna where the E-Field and H-Field are out of phase with one another[5].

$$Reactive\ Near\ Field\ Region\ <\ 0.62\sqrt{\frac{D^3}{\lambda}}$$

The radiative near field is indeed the region among reactive and radiative fields in which electromagnetic waves begin their transition from reactive to radiative fields. It is provided by[5]

$$0.62\sqrt{\frac{D^3}{\lambda}} < \boldsymbol{Radiative\ Near\ Field\ Region} < \frac{2D^2}{\lambda}$$

The far field region is located beyond an antenna and follows the radiative near field. Its distance equation[5]

$$Far\ Field\ Region > \frac{2D^2}{\lambda}$$

All of the regions are depicted in the image below,

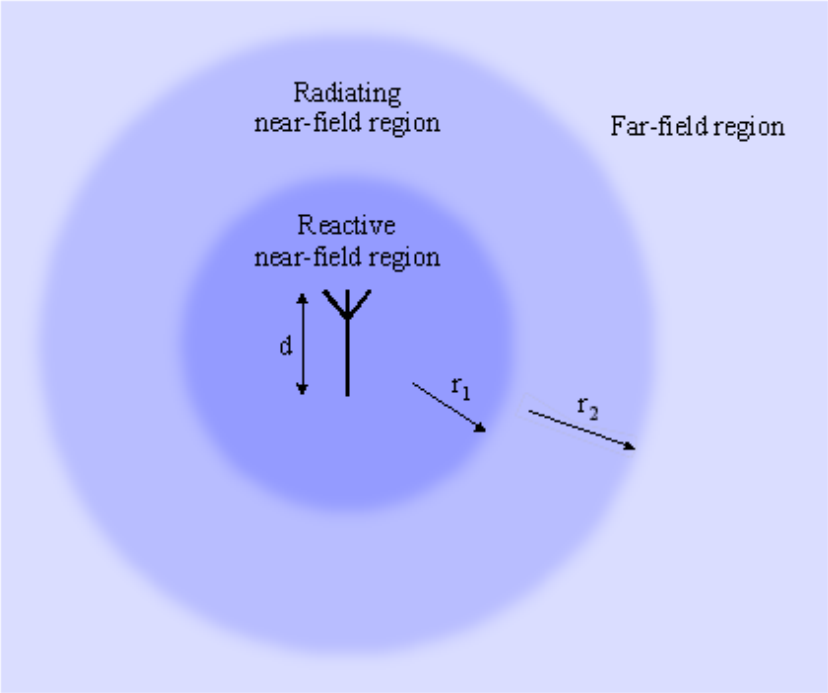


**Figure 4 2.1.1 (c): Fields's representation of an antenna [3]**

The antenna average power is represented by[3]:

$$P_{rad} = P_{av} = \oiint_s \boldsymbol{W}_{rad} \,.\, d\boldsymbol{S} = \oiint_s \mathbf{W}_{\mathrm{av}} \,.\, \bar{\mathrm{n}}\, da$$

$$= \frac{1}{2} \oiint_s Re[\mathbf{E} \times \mathbf{H}^*] \,.\, d\mathbf{S}$$

### *2.1.2 Antenna Directivity:*

The term "directivity" refers to an antenna's ability to radiate and gain more radiation in a certain direction. Increased directivity implies that the beam will travel a longer distance. It is expressed in decibels (dB)[6].

In mathematical form,

$$D = \frac{U}{U_0} = \frac{4\pi U}{P_{\mathrm{rad}}}$$

The direction in which the greatest amount of radiation is emitted (highest directivity), given as[3],

$$D_{\max} = D_0 = \frac{U|_{\max}}{U_0} = \frac{U_{\max}}{U_0} = \frac{4\pi U_{\max}}{P_{\text{rad}}}$$

Where,

$D$ = directivity (dimensionless)

$D_0$ = maximum directivity (dimensionless)

$U$ = radiation intensity (W/unit solid angle)

$U_{max}$ = maximum radiation intensity (W/unit solid angle)

$U_0$ = radiation intensity of isotropic source (W/unit solid angle)

$P_{rad}$ = total radiated power (W)

It is self-evident from the preceding equation that the directivity of an isotropic source is unity, as U, Umax, and U0 are all equal[3].

Antenna efficiency accounts for all the losses that can occur such as dielectric, VSWR and many more.

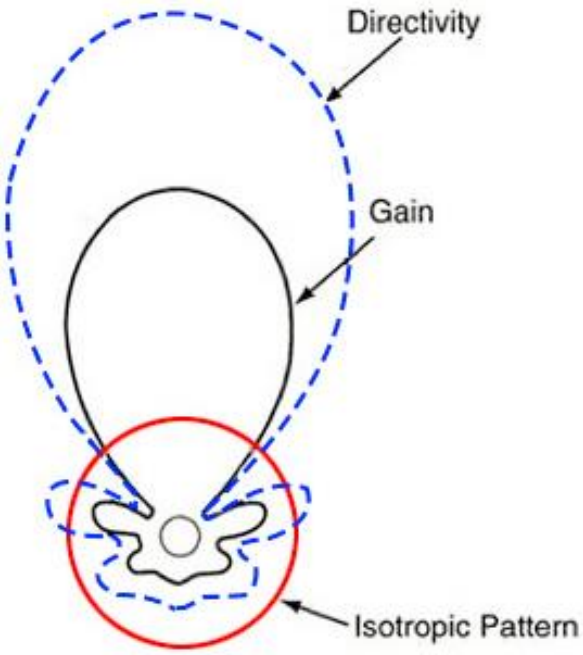


**Figure 5 2.1.2: Isotropic antenna pattern [5]**

Antennas with higher directivities are frequently employed in more fixed sites, like radio communication and television satellites, where data must be carried over longer distances.

### *2.1.3 Antenna gain:*

Gain is depending on the antenna's efficiency and directivity. Thus, gain is defined as ratio of the power density of the antenna at a given distance to its input power. An antenna's gain (in a particular direction) is given as "the ratio of the intensity in a particular direction to the radiation intensity that would be attained if the antenna absorbed all power isotropically radiated."[3] This can be stated mathematically as,

$$\text{Gain} = 4\pi \frac{\text{radiation intensity}}{\text{total input (accepted) power}} = 4\pi \frac{U(\theta,\phi)}{P_{in}} \qquad \text{(dimensionless)}$$

In above equation,

U = radiation density,

$P_{in}$ = total input power.

Relative gain is frequently used and is defined as "the ratio of the power gain in a given direction to the power gain in the referenced direction of a reference antenna." Both antennas must share the same power supply[3].

In case of lossless isotropic antenna, the equation of gain becomes

$$G = \frac{4\pi U(\theta, \phi)}{P_{\text{in}}}$$

As a result, when no direction is specified, the direction of strongest radiation is used to calculate the power gain.

### *2.1.4 Antenna efficiency:*

The antenna's efficiency can be defined as the sum of loss at the input terminal and within the antenna's structure. It can be seen from figure below[3]

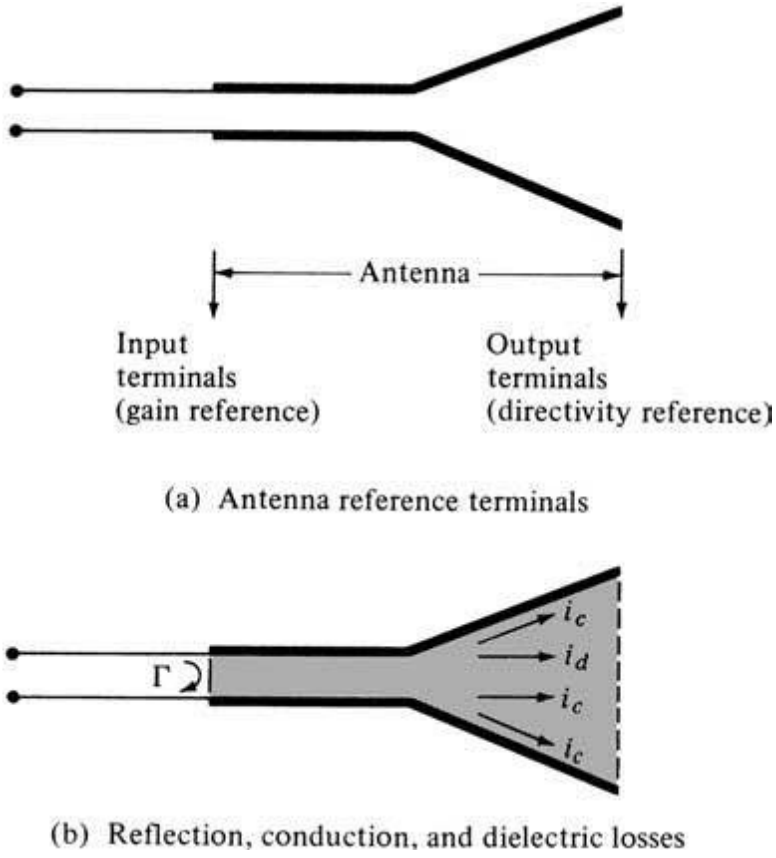


**Figure 6 2.1.4 Antenna's reference terminals, losses, reflection, and conduction [3]**

As a result, total efficacy can be expressed as[3],

$e_0 = e_r\, e_c\, e_d$

where,

$e_0$= *total effieciency (dimensionless)*

$e_r$ = *reflection (mismatch effieciency)*

$e_c$ = *conduction effieciency (dimensionless)*

$e_d$ = *dielectric effieniency*

$e_c$ and $e_d$ both can be computed experimentally but are difficult to compute.

### *2.1.5 Polarization:*

Since we understand that an antenna's electromagnetic wave is indeed a vector quantity in terms of time and space. This vector quantity is of an electromagnetic wave in medium it is radiated is also called polarization[7]. Polarization is classified into three types: linear, circular, and elliptical. When an electromagnetic wave propagates vertically or horizontally as a function of time and space, it is said to be linearly polarized. Circularly polarized waves propagate in circles, and so fall into two categories: right-hand circular polarization (RHCP) and left-hand circular polarization (LHCP). Elliptical polarization occurs when radio waves have a phase and magnitude discrepancy[7].

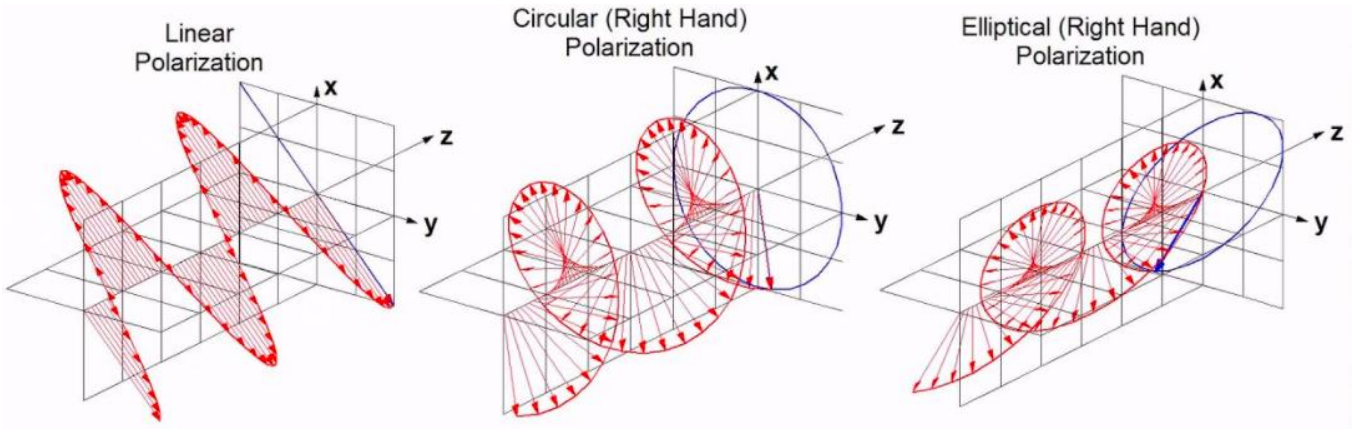


**Figure 7 2.1.5: Polarization of an antenna [7]**

### 2.1.5 Bandwidth:

The antenna bandwidth is the frequency range over which it works as specified[3].

$$Bandwidth$$
$$BW = f_{max} - f_{min}$$

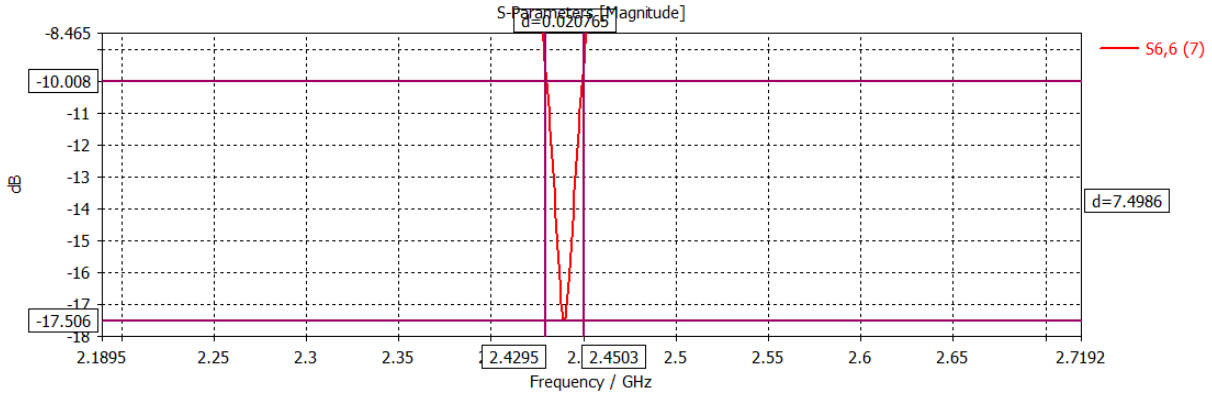


A broadband antenna's bandwidth is commonly defined as the ratio of its permissible upper-to-lower operating frequencies. For example, a 10:1 bandwidth indicates that the topmost frequency is 10 times higher than that of the bottom frequency. The bandwidth of the narrowband antenna is measured as a proportion of the frequency variation (upper minus lower) between the bandwidth's center frequency and the frequency variations (upper minus lower). For example, a 5% bandwidth indicates that the maximum frequency difference permitted for functioning is 5% of bandwidth's center frequency. [3].

Since the characteristics of are constantly varying depending on the frequency, bandwidth cannot be characterized. Therefore, the specification is defined for each case uniquely to meet the desired outcome.

### 2.1.6 Input Impedance:

The word "input impedance" refers to "the impedance produced by an antenna at its terminals, the voltage to current ratio at a pair of terminals, or the ratio of the

corresponding components of the electric as well as magnetic fields at a point". Now considering terminal, a, and b,[3]

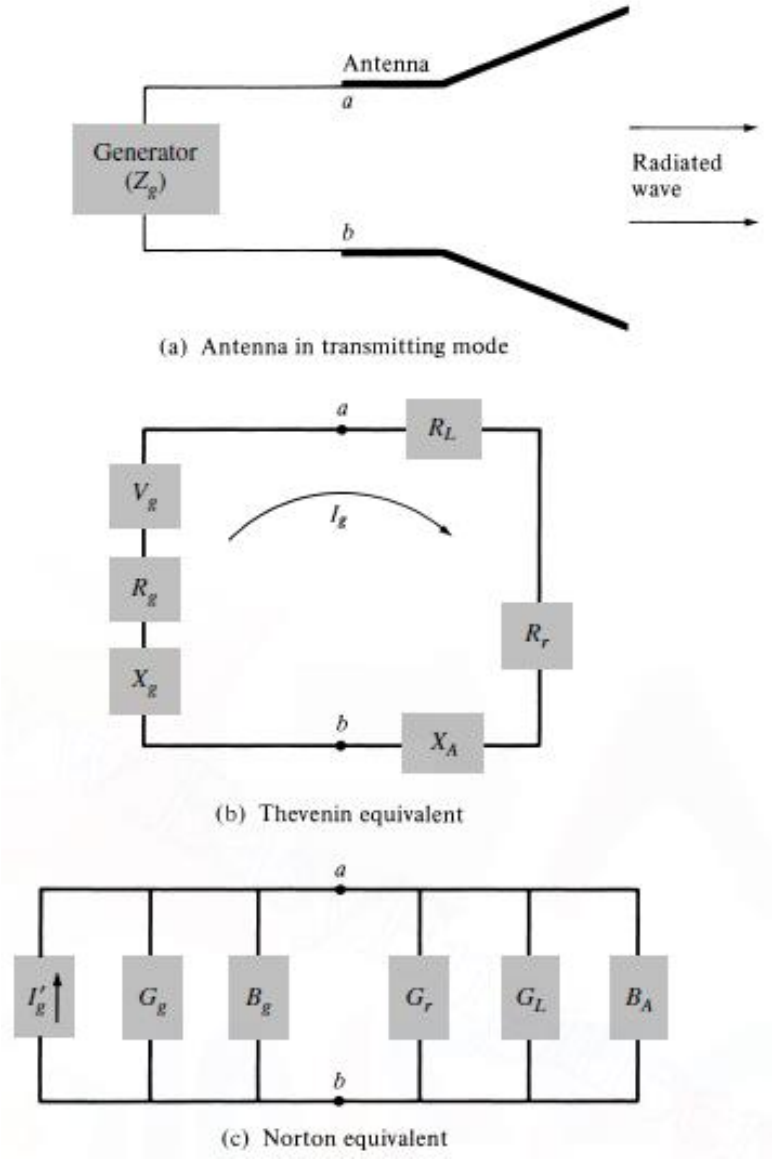


**Figure 8 2.1.6 Examples of different transmitting antennas [3]**

At these terminals, the voltage-to-current ratio is defined as[3]

$$Z_{AI} = R_{AR} + jX_{AR}$$

Where,

$Z_{AI}$ = antenna impedance (ohms)

$R_{AR}$ = antenna resistance (ohms)

$X_{AR}$ = antenna reactance (ohms)

Now, for the above equation, the resistive part consists of two components[3],

$$R_A = R_{ar} + R_{al}$$

Where,

$R_{ar}$ = Antenna radiation resistance

$R_{al}$ = Antenna loss resistance

## 2.2 Antenna Beamforming:

Beamforming is a method that is used in the latest generation of mobile communication's smart antennas. Which operates on the fundamental idea of directing the radio signal's beam in a specific direction instead of transmitting the signal across all directions[8].

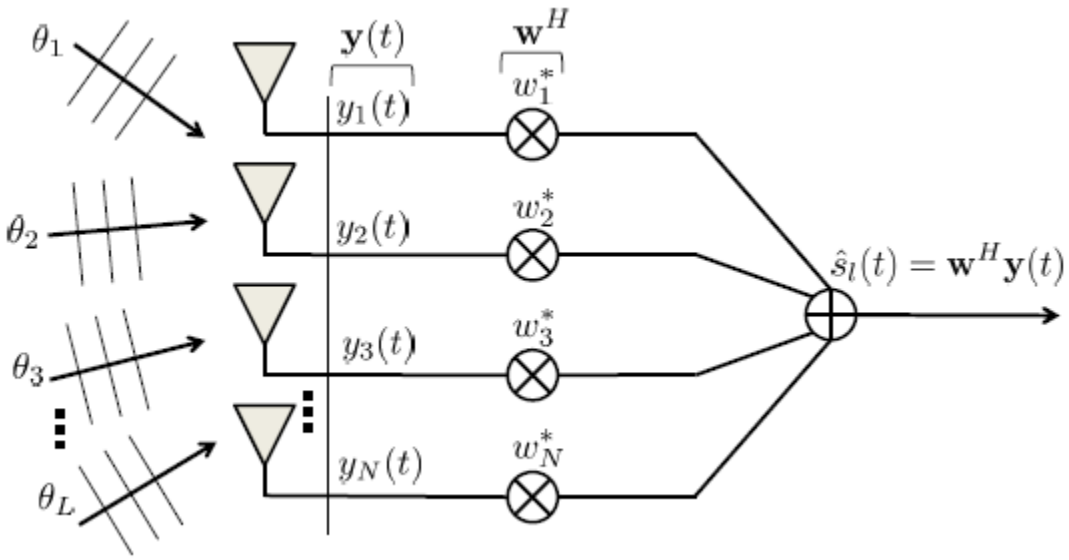


**Figure 9 2.2: Beamforming schematic Diagram [3]**

This technique is common practice from a while now in both radar and mobile communication. With the time this technique is becoming more and more critical and therefore different methods are being use for its further improvements.

### *2.2.1 Principles of Beamforming:*

Antenna with beamforming consists of a set of smaller antennas that work in concert to transmit amplitude and phase signals. By adjusting the phase of each individual antenna, overall phase of the beam can be adjusted to suit the application[9].

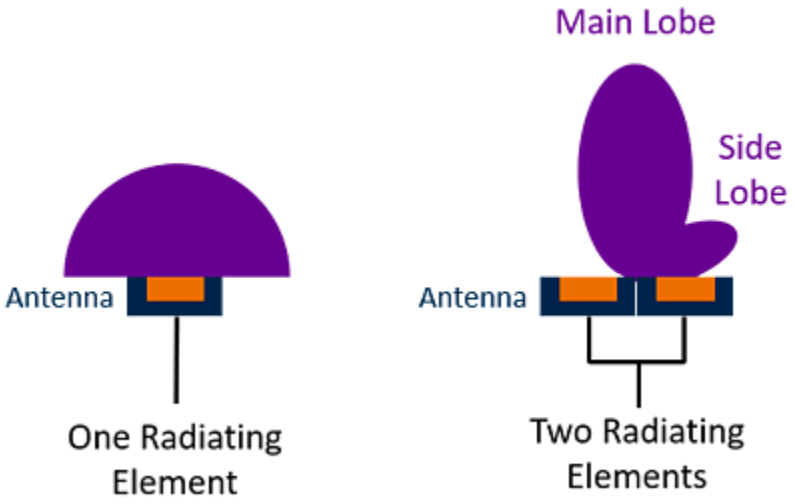


**Figure 10 2.2.1.1: Single and double antenna radiating pattern [5]**

Another main component includes the use of MIMO (multiple input multiple output) technique which is around telecommunication technology since 3G. It enables the reception or transmission of signals via multiple antennas. The primary advantage of this technology is the increased data rate[9]. More on this later.

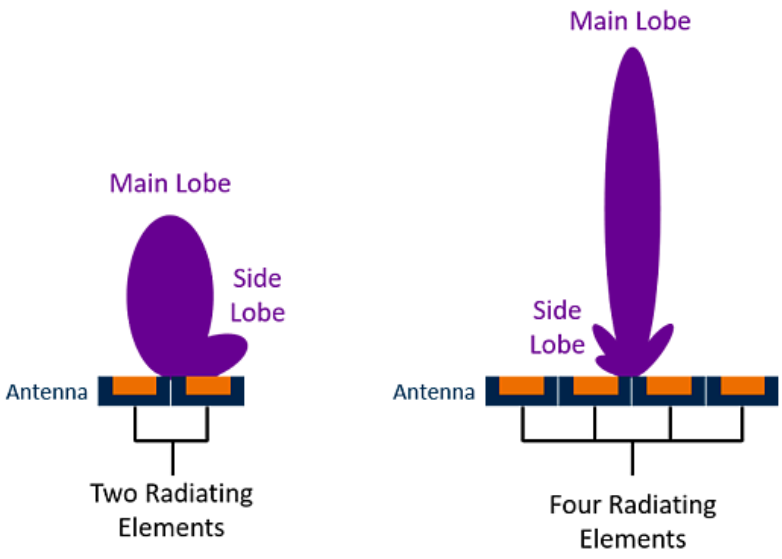


**Figure 11 2.2.1.2: Two and four elements radiating pattern [5]**

As illustrated above, the signal beam grows denser and narrower as the numbers of elements increases. One disadvantage of this approach is that it results in the formation of side lobes. These are essentially undesired signals that exist near the main lobe of our signal. The intensity of such signals can be reduced by increasing the number of antenna elements and optimizing them.

### *2.2.2 Beam Steering and Beam Switching:*

The beam steering approach is accomplished by changing the phase of antenna patch. This phase shift enables the array of elements to aim a beam in a specific direction[10].

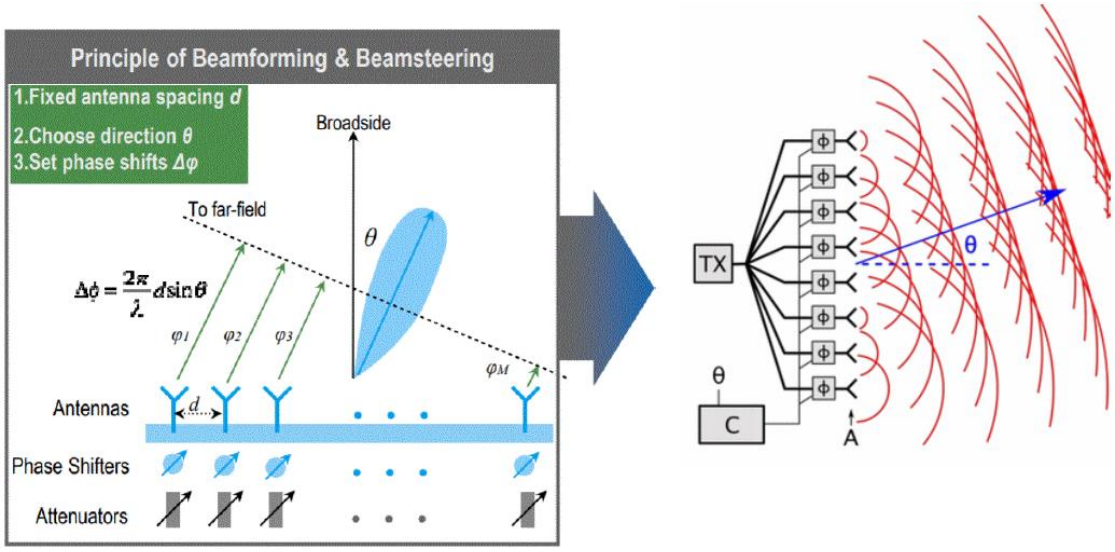


**Figure 12 2.2.2.1: Beam steering and beam switching [7]**

As can be seen, an array of elements can utilize a single common frequency to direct a beam, or it can use several more frequencies to serve multiple users via sperate beams. In the instance of beam switching, the direction in which the beam can be switched is determined by the antenna arrangement. This function is meant to protect the signal and improve its usability[9].

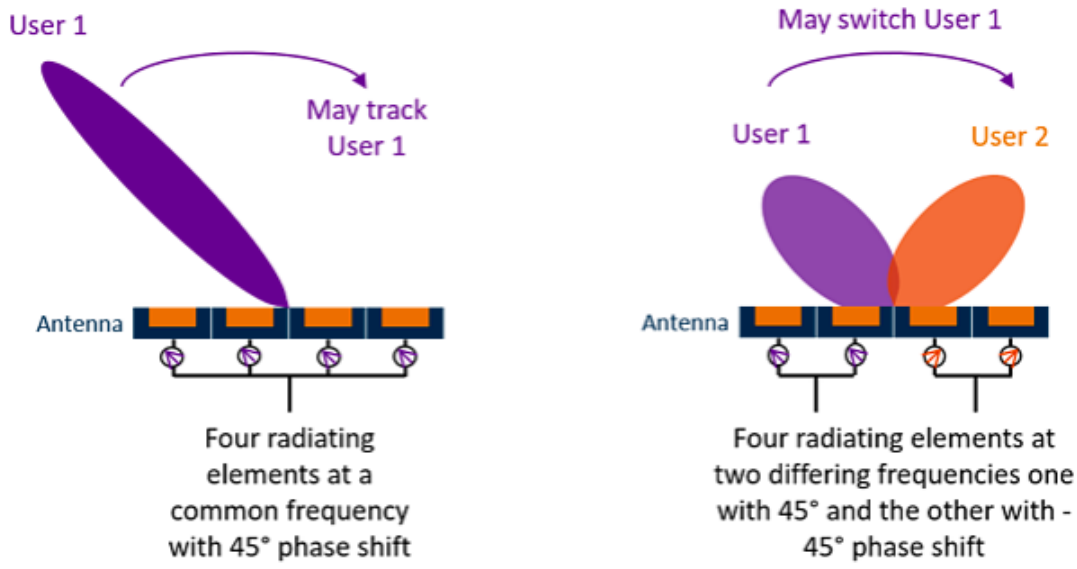


**Figure 13 2.2.2.2: Radiating patterns of common frequency and differing frequencies [5]**

By beam steering an antenna, we potentially can increase its gain and, to a large extent, eliminate interference. Generally, these antennas are capable of delivering 360 degrees of angular coverage[11]. Additionally, they are capable of providing limited angular coverage of around 45 degrees by combining 'm' equally spaced directed beams [11].

### *2.2.3 Beamforming for Capacity and Coverage:*

While adding antennas increases gain, the number of layers that can be spatially multiplexed using MIMO is limited at the user end[10]. As a result, extra antennas are employed to enhance coverage[10].

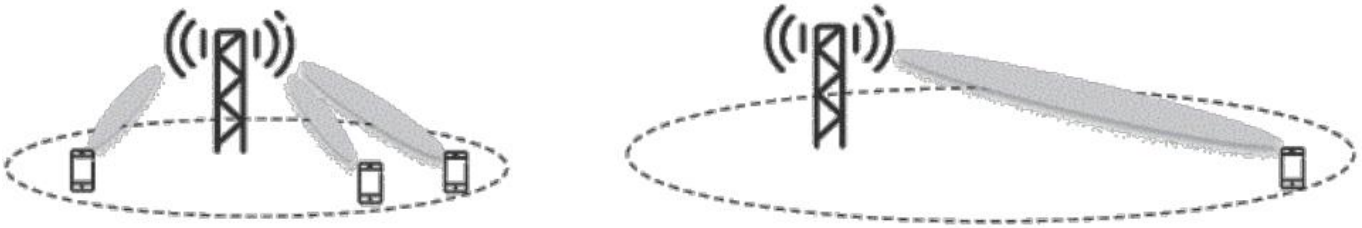

**Figure 14 2.2.3: Beamforming for capacity and coverage [3]**

This approach is more effective when operating at higher frequencies when attenuation is greater. Beamforming is a critical technique for enhancing the coverage of a network.

## 2.3 Types of Antenna array:

Antenna array are different from one another based on their radiation patterns and radiating elements used. The use of antennas in modern mobile communication enables us to achieve superior signal quality, more coverage, decreased channel interference, increased efficiency, and beam directing capabilities[12]. Some of the different types of antenna array are explain below.

### 2.3.1 Linear Array Antenna:

When elements of antenna are consistently aligned, the antenna is referred to as a linear array antenna. The elements of the antenna are uniformly spaced apart[12].

In order to understand, let us consider an example of N- elements[13].

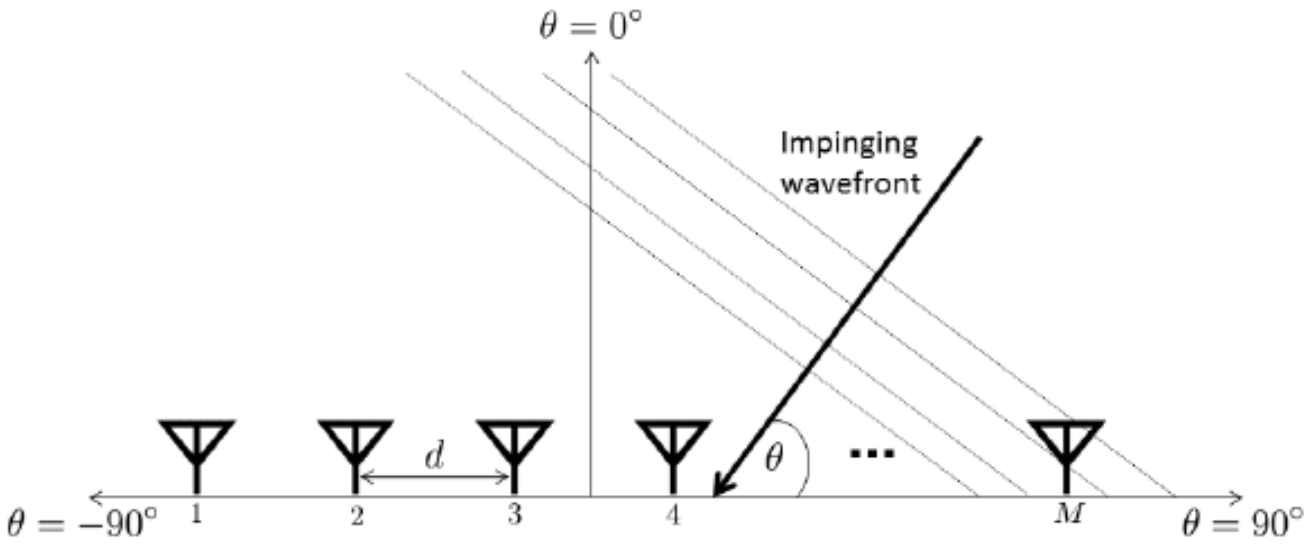


Figure 15 2.3.1: Linear array of M-elements [3]

In the above figure it can be seen that elements are separate by inter-elements spacing d. Since we assume that it is a uniform array with which means that all the elements have identical magnitude with a progressive phase and are isotropic as well.

The array factor of each element in the N-dimensional linear array is equal to [3]:

$$\mathrm{AF} = 1 + e^{+j(kd\cos\theta+\beta)} + e^{+j2(kd\cos\theta+\beta)} + \cdots + e^{j(N-1)(kd\cos\theta+\beta)}$$

$$\mathrm{AF} = \sum_{n=1}^{N} e^{j(n-1)(kd\cos\theta+\beta)}$$

By neglecting the phase factor, the equation of AF becomes[3]:

$$\mathrm{AF} = \sum_{n=1}^{N} e^{j(n-1)\psi}$$

Where, $\psi = kd\cos\theta + \beta$.

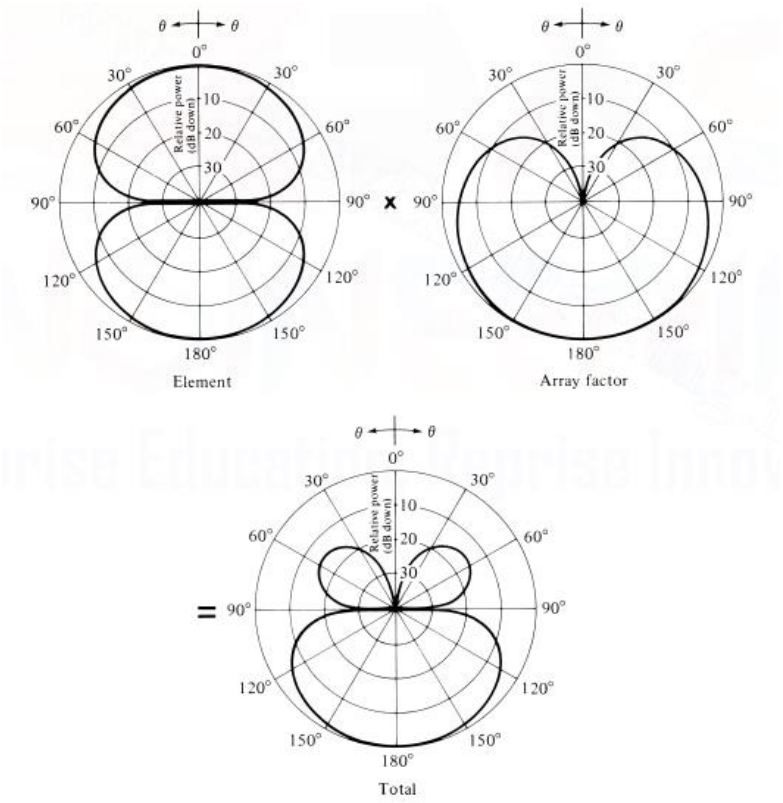


**Figure 16 2.3.1 Multiplication pattern of array factor, element, and total of 2-D array [3]**

It can be concluded that in order to achieve maximum radiation, the array elements must be consistent with array factor and then the direction can be managed by the array factor.

#### *2.3.1.1 Narrowband Signal Model:*

Given that the array's signal is a narrowband signal, its complex envelope is denoted by [13]:

$$x(t) = s(t)\, e^{j2\pi f_c t}$$
$$\Downarrow$$
$$x(t-\tau) \simeq s(t)\, e^{j2\pi f_c (t-\tau)}$$

Due to the fact that the envelope does not really change during certain cycles of sinusoidal waveforms. As a result, the signal received at the mth antenna becomes [13]:

$$y_m(t) = s(t)\, e^{j2\pi f_c \frac{a}{c}(m-1)\sin\theta}\, e^{j2\pi f_c t} + n_m(t)$$

Now by arranging each antenna as M x 1 vector, the steering vector can be represented as[13]:

$$\mathbf{a}(\theta) = \begin{bmatrix} 1 \\ e^{j2\pi \frac{d}{\lambda}\sin\theta} \\ \vdots \\ e^{j2\pi \frac{d}{\lambda}(M-1)\sin\theta} \end{bmatrix}$$

$$\mathbf{y} = s \cdot \mathbf{a}(\theta) + \mathbf{n}$$

And the spacing of an antenna becomes[13]:

$$d \leq \frac{\lambda}{2}$$

### *2.3.2 Planar Array Antenna:*

As illustrated in the picture, a planar array configuration has N elements along the y-axis and M elements along the x-axis. The distance among elements is expressed by dx along the x-axis and by dy along the y-axis. All distances are equal. A planar array is essentially a collection of several linear arrays[3].

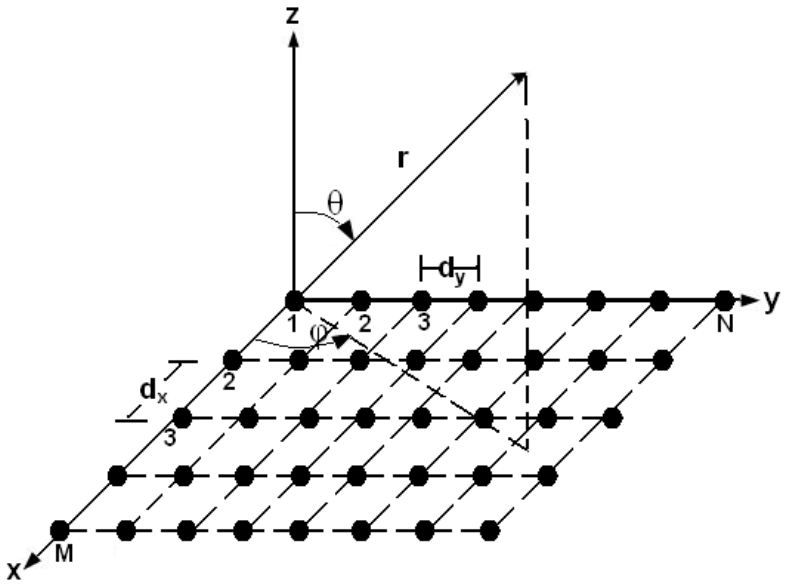


**Figure 17 2.3.2.1: Planar array of MxN elements [3]**

Consider the situation of an 8x8 uniform planar array with dx=dy=λ/2 spacing[13],

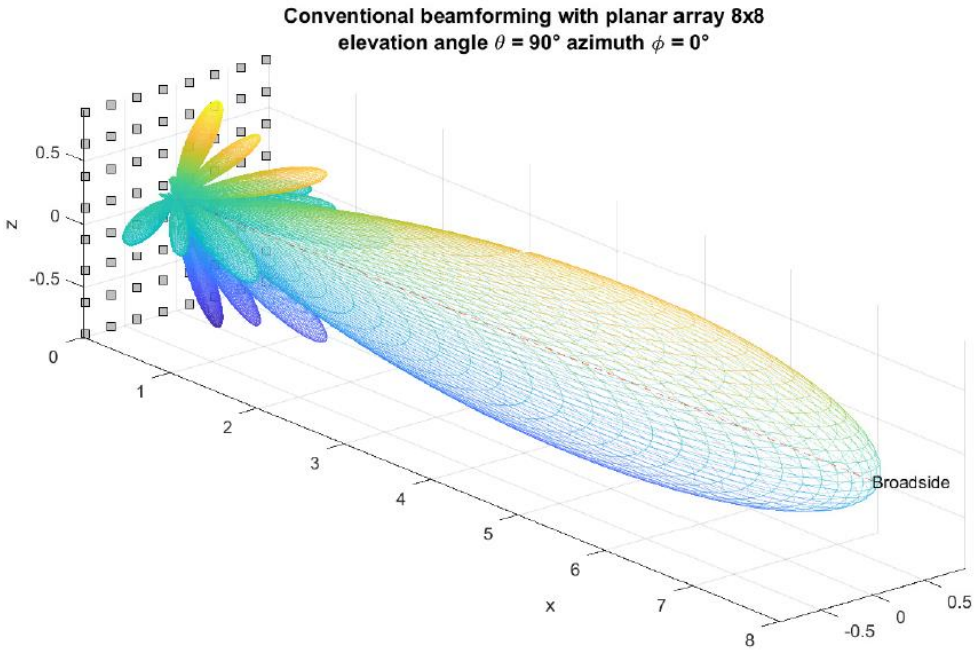


(b)

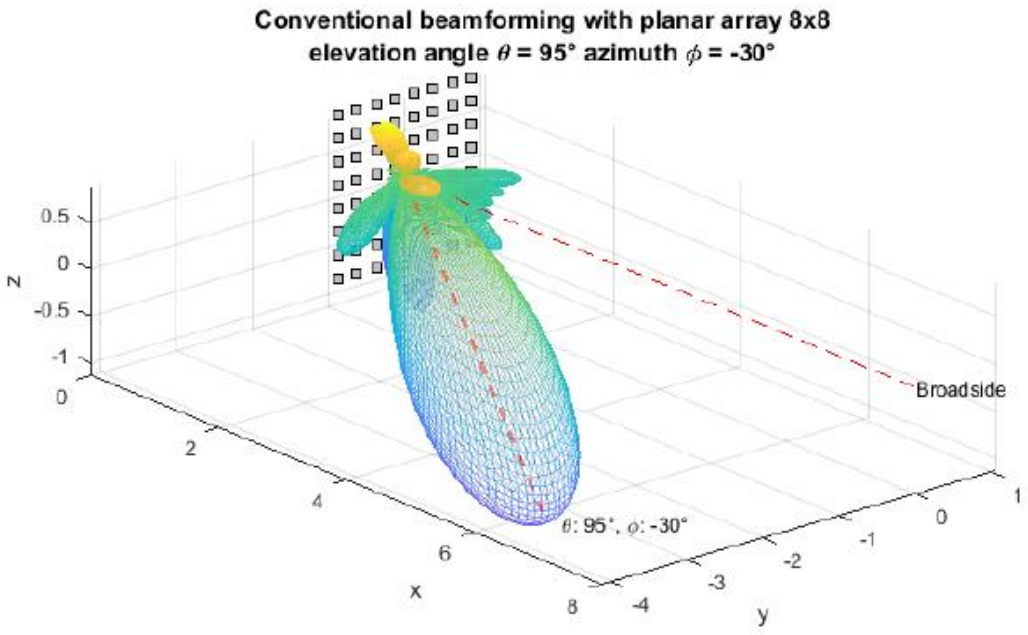


(c)

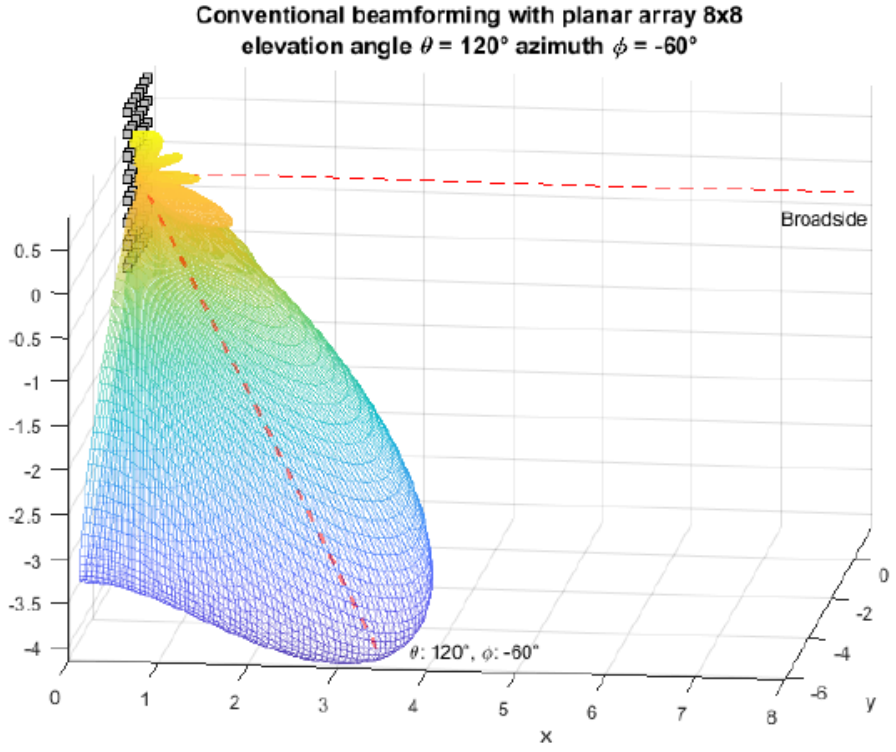


(d)

**Figure 18 2.3.2: 3-D representation of planar array radiation pattern [8]**

As the elevation angle increases, the array's vertical resolution degrades noticeably.

Now, because the design principle of a planar array antenna is indeed very identical to that of a linear array antenna, the array factor of the planar array antenna may be derived by multiplying the linear arrays along the x-axis and y-axis[3].

$$AFplanar = (AFx).(AFy)$$

$$\Downarrow$$

$$AF = \left(\frac{sin(N\psi x/2)}{N\,sin(\psi x/2)}\right)\left(\frac{sin(M\psi y/2)}{M\,sin\,sin(\psi y/2)}\right)$$

Where,

$\psi x = kdx\ sin\ \theta\ cos\ \varphi + \xi x$

$\psi y = kdy\ sin\ \theta\ cos\ \varphi + \xi y$

By employing the linear array steering vector's formulae for x-axis and y-axis[13],

$$\xi_x = 2\pi\frac{d_x}{\lambda}\cos\ \theta$$

$$\xi_y = 2\pi\frac{d_y}{\lambda}\sin\ \theta\sin\ \phi$$

Both axes now have a steering vector[13],

$$\mathbf{a}_x = \begin{bmatrix} 1 \\ e^{j\xi_x} \\ \vdots \\ e^{j\xi_x(M-1)} \end{bmatrix} \mathbf{a}_y = \begin{bmatrix} 1 \\ e^{j\xi_y} \\ \vdots \\ e^{j\xi_y(N-1)} \end{bmatrix}$$

As a result, we obtain the planar steering vector by multiplying the above steering vector by the Kronecker product[13],

$$\mathrm{a}(\theta,\phi) = \mathbf{a}_z \otimes \mathbf{a}_y = \begin{bmatrix} 1 \\ e^{j(\xi_z+\xi_y)} \\ \vdots \\ e^{j[\xi_z(M-1)+\xi_y(N-1)]} \end{bmatrix}$$

### *2.3.3 Circular Array Antenna:*

The N elements of the antenna are placed in a ring shape and are evenly spaced apart in a circular array configuration. One of the most significant features of this design is its ability to perform 360° beam scanning by adjusting the beam width or side lobe levels slightly.

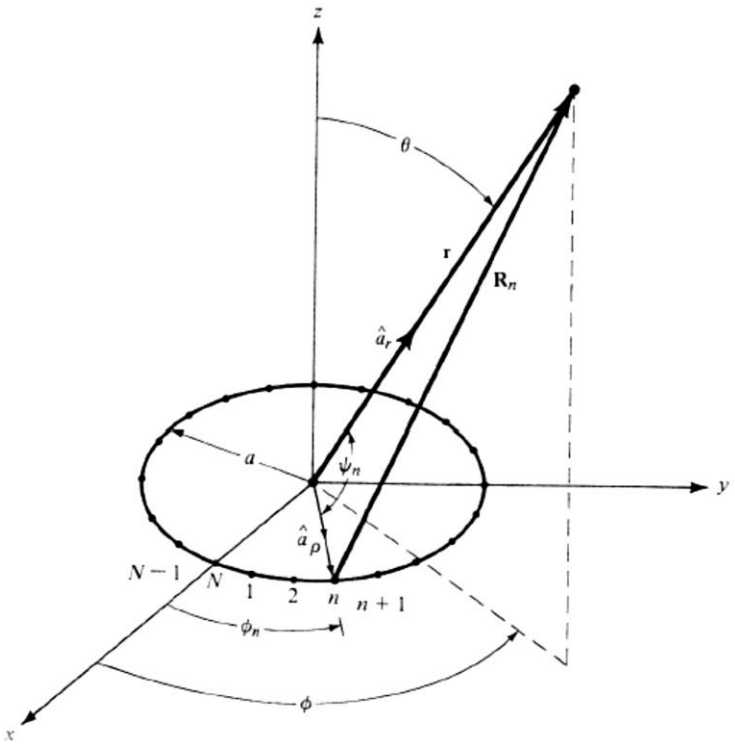


**Figure 19 2.3.3.1: N elements Circular array antenna [3]**

3D representation of 32 elements of circular array antenna is given by[13],

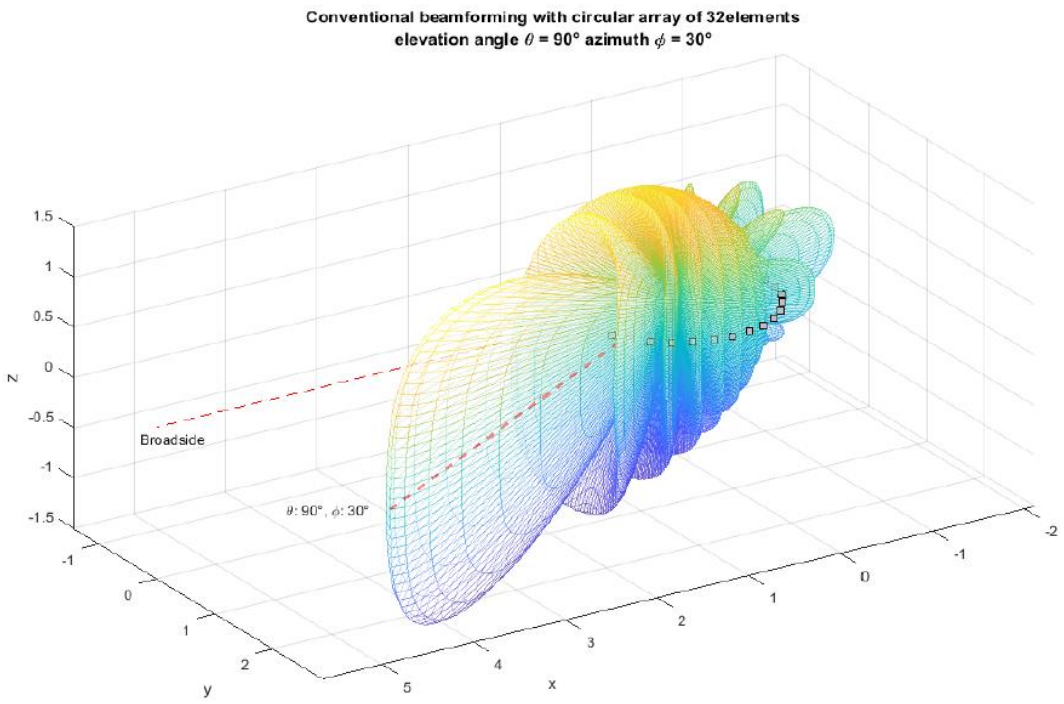


**Figure 20 2.3.3.2: 3-D representation of circular array radiating pattern [8]**

Now, referring to the preceding illustration, the radius of the circle in the normalization field can be stated as[3]

$$E_n = \sum_{n=1}^{N} a_n \frac{e^{-jR_u}}{R_n}$$

Where,

$a_n$ represents the nth element's excitation coefficient.

The distance between the nth element and the observation point is denoted by $R_n$, which can be represented as[3],

$$R_n = r - a\sin\,\theta\cos\,(\phi - \phi_n)$$

Taking into consideration $R_n \cong r$, normalization field equation becomes[3],

$$E_n(r,\theta,\phi) = \frac{e^{-jkr}}{r}\sum_{n=1}^{N} a_n e^{jka\sin\,\theta\cos\,(\phi-\phi_n)}$$

And,

$$E_n(r,\theta,\phi) = \frac{e^{-jkr}}{r}[AF(\theta,\phi)]$$

Circular array factor is represented by $AF(\theta,\phi)$ whose simplified equation is given by[3],

$$AF(\theta,\phi) = \sum_{n=1}^{N} I_n e^{j[ka\sin\,\theta\cos\,(\phi-\phi_n)+\alpha_n]}$$

Where,

$\alpha_n$ is the phase excitation of *n*th element. Main beam can be directed by changing the phase excitation, which is represented as[3],

$$\alpha_n = -ka\sin\,\theta_0\cos\,(\phi_0-\phi_n)$$

Therefore, the *AF* can be written as[3],

$$AF(\theta,\phi) = \sum_{n=1}^{N} I_n e^{jka[\sin\,\theta\cos\,(\phi-\phi_n)-\sin\,\theta_0\cos\,(\phi_0-\phi_n)]}$$

$$AF(\theta,\phi) = \sum_{n=1}^{N} I_n e^{jka(\cos\,\psi_n-\cos\,\psi_0)}$$

Where,

$$\cos\psi_n = [\sin\theta\cos(\phi-\phi_n)]$$

$$\cos\psi_{0_n} = [\sin\,\theta_0\cos\,(\phi_0-\phi_n)]$$

As the array's radius increases, the uniform circular array's directivity reaches the value of N, the array's element count.

From the observation angle pair (θ, $\phi$), we have phase term equation[13],

$$\xi_n = \frac{2\pi}{\lambda}R\sin\,\theta\cos\,\left(\phi-2\pi\frac{n}{N}\right)$$

By using the above equation, steering vector for the uniform circular array becomes[13],

$$\mathbf{a}(\phi,\theta) = \begin{bmatrix} e^{j\frac{2\pi}{\lambda}R\sin\,\theta\cos\,\phi} \\ e^{j\frac{2\pi}{\lambda}R\sin\,\theta\cos\left(\phi-\frac{2\pi}{N}\right)} \\ \vdots \\ e^{j\frac{2\pi}{\lambda}R\sin\,\theta\cos\left(\phi-2\pi\frac{N-1}{N}\right)} \end{bmatrix}$$

And the antenna spacing design becomes[13],

$$d_{arc} \triangleq \frac{2\pi R}{N} \leq \frac{\lambda}{2} \Longrightarrow R \leq \frac{N\lambda}{4\pi}$$

### *2.3.4 Cylindrical Array Antenna:*

A cylindrical array is made up of N-elements organized in a circular configuration and M-elements arranged in a cylindrical arrangement[14]. These M-elements are linear array with each having radius a as shown in figure below.

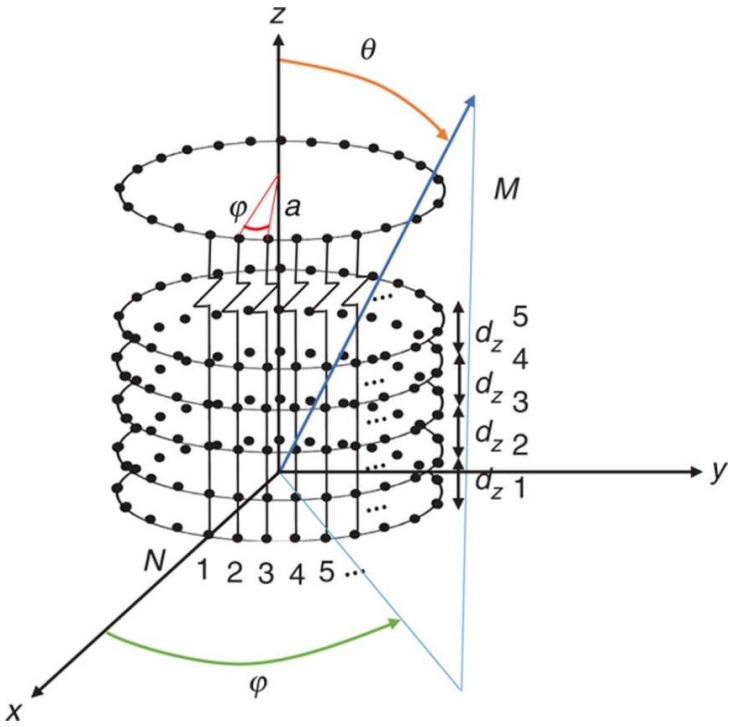


**Figure 21 2.3.4.1: NxM element cylindrical array antenna [3]**

The primary advantage of adopting these circular arrays is that they provide symmetrical radiation patterns in radar technology[14].

Radiation pattern of these elements can be written as[15]:

$$E(\theta,\varphi) = \mathrm{e}^{-\mathrm{j}((M-1)/2)\psi_Z} \sum_{m=1}^{M} \mathrm{e}^{j(m-1)\psi_Z} \times \sum_{n=0}^{N-1} a_{mn} f_n(\theta, \varphi - n\Delta\varphi) \mathrm{e}^{jka(\sin\,\theta\cos\,(\varphi - n\Delta\varphi))}$$

Where,

$$k = 2\pi / \lambda$$

$f_n(\theta,\varphi)$ Are the elements radiation patterns, $a_{mn}$ is amplitude weight applied to the *mnth* element.

The three-dimensional representations of 32 elements every circle in a four-ring structure is provided by [8],

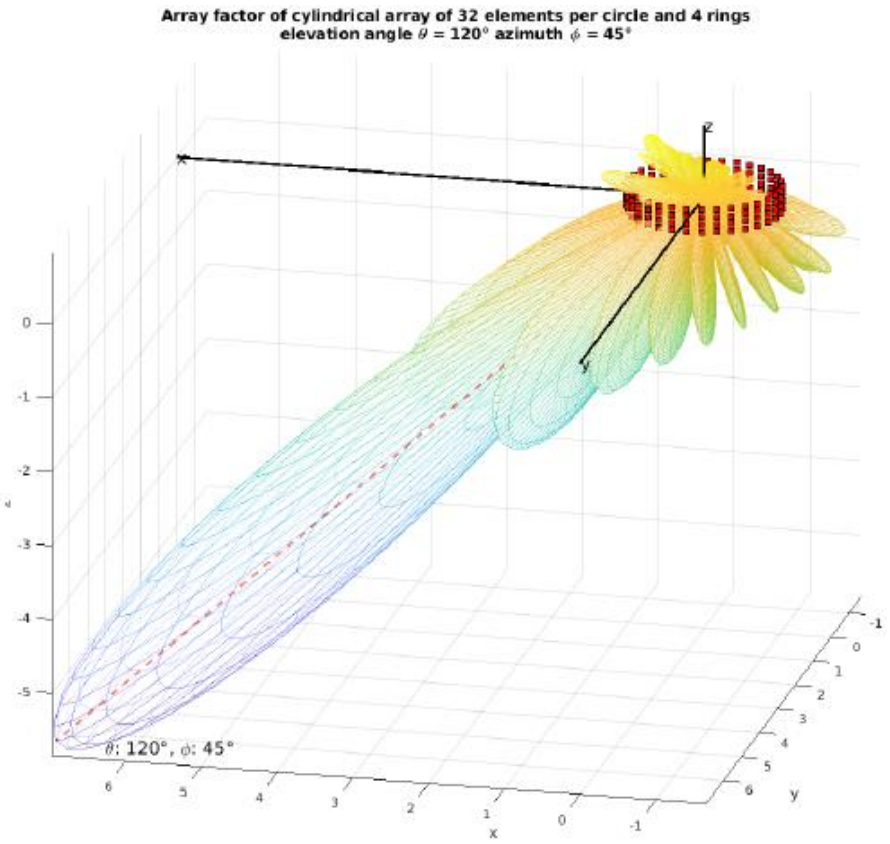


**Figure 22 2.3.4.2: 3-D representation of 32x4 elements cylindrical array radiating pattern [8]**

### *2.3.5 Conformal Array Antenna:*

The conformal antenna is one that adheres to a specified shape. The purpose is to integrate the antenna into the construction while minimizing friction. Additionally, the objective of antenna integration may be to make the antenna less visible[16]. According to the IEEE definition of antenna terms “An antenna [an array] that conforms to a surface whose shape is determined by considerations other than electromagnetic, for example, aerodynamic or hydrodynamic”[16]

Conformal antennas are often cylindrical or spherical in shape due to their primary applications in military, aircraft, and high-speed trains.

The traditional solution in mobile communication is to use three sperate antennas, each covering 120 degrees in azimuth[17]. Instead of three separate antennas, modern technology allows for the use of a single cylindrical or circular antenna, which is more efficient and less expensive[18].

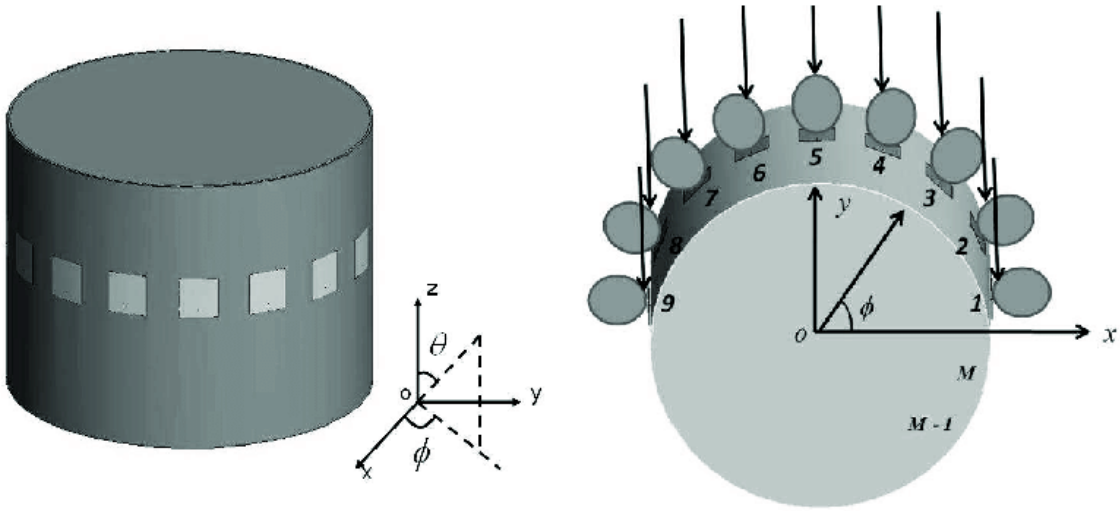


**Figure 23 2.3.5.1: Conformal cylindrical antenna [16]**

Another application of conformal antennas is in modern aircraft[16],

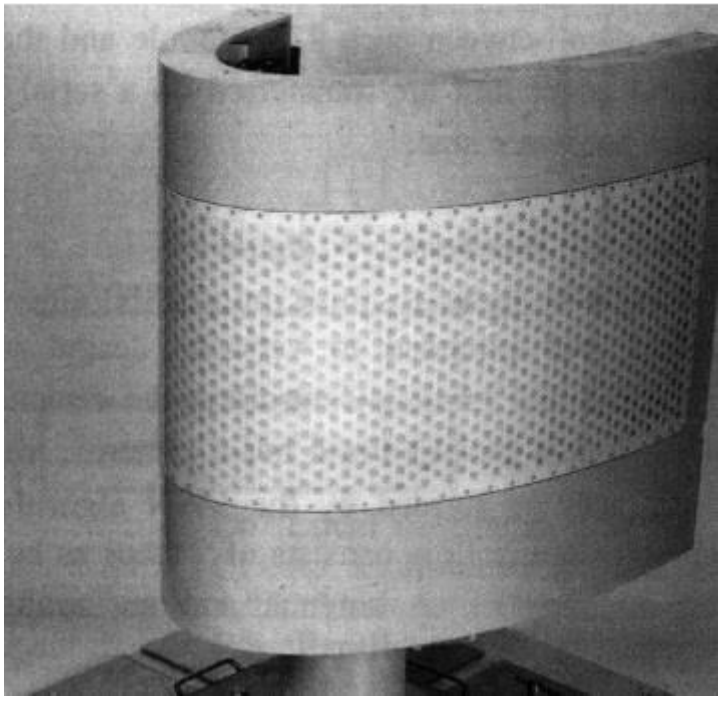

**Figure 24 2.3.5.2: Conformal antenna for aircraft wing integration [16]**

When conformal antennas are operated, the substrate surface changes with time, resulting in radiation distortion in non-planar orientations. Its problem can be solved by the use of a technique known as phase steering[17].

# Chapter 3: Design and Simulation

## *3.1 Simulation tool:*

The CST microwave studio tool is used to design and simulate antennas. It encompasses equipment for the design, recreation, and development of a diverse range of devices, ranging between fixed through optical and electrically big to tiny scale. It is not limited to electromagnetic waves, but it also takes into account the circuit's thermal and mechanical effects. CST microwave studio offers a variety of experimentation settings, including virtual design modeling prior to physical preliminary work and simplifying or advancement instead of experimentation. Execution of gadgets can be facilitated, potential inconsistency concerns can be identified and mitigated prior to the design phase, the number of physical models needed can be reduced, and the risk of test disappointments and reviews may be reduced[19].

## *3.2 Cylindrical Conformal Array:*

An antenna [an array] that adapts to a surface governed by factors other than electromagnetics, such as aerodynamic or hydrodynamic considerations[20]. A conformal array antenna is one that has a radiating surface that is a cylinder, sphere, or cone. The shape of the antennas may be dictated by a specific electromagnetic requirement, like antenna beam design and/or angular coverage[20]. Cylindrical conformal antennas are used in telecommunication base stations because they appear to be less congested than conventional sectorial antennas.

Due to the fact that these types of antennas conform to the geometry of the platform, their performance but also radiation patterns are significantly different than those of typical planar array antennas[21].

## *3.3 Design of conformal array antenna:*

Three components comprise the antenna design: a rectangular patch element, a dielectric substrate material, and a ground plane. The rectangular patches and ground are both

made of copper. The thickness of dielectric substrate used is 0.8mm of rogers RT 5880, on this in next section. Design is of 4x16 configuration as shown below,

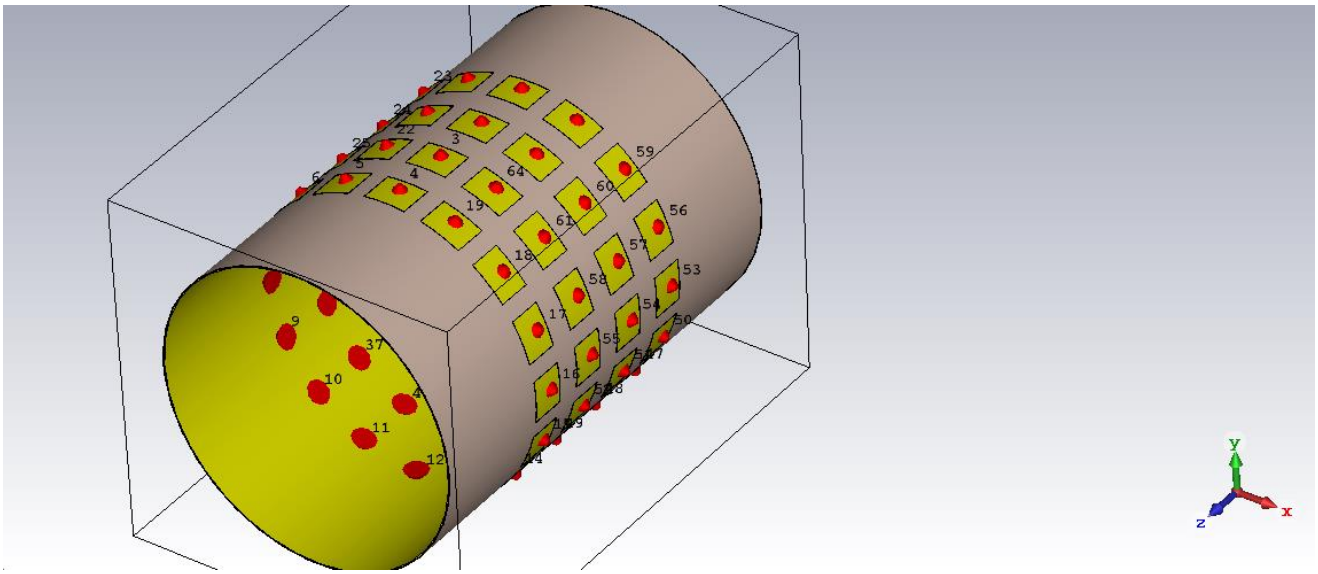


**Figure 25 3.3: Conformal antenna of 4x16 configuration**

All patches are equally distance from one another and the equally distance from both end of cylinder.

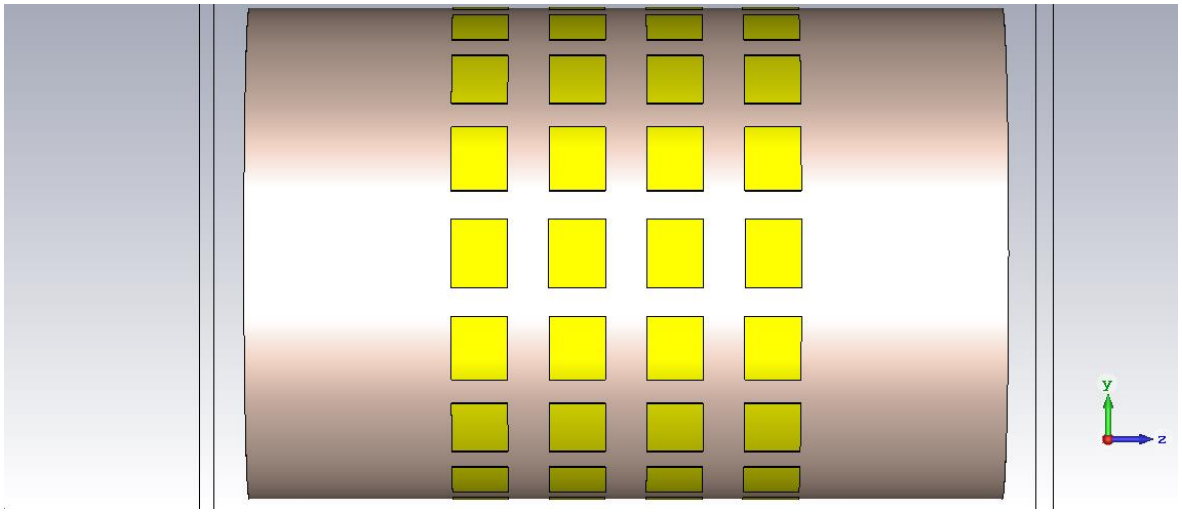


**Figure 26 3.3: Equally spaced elements**

Single element rectangular patch can be seen below,

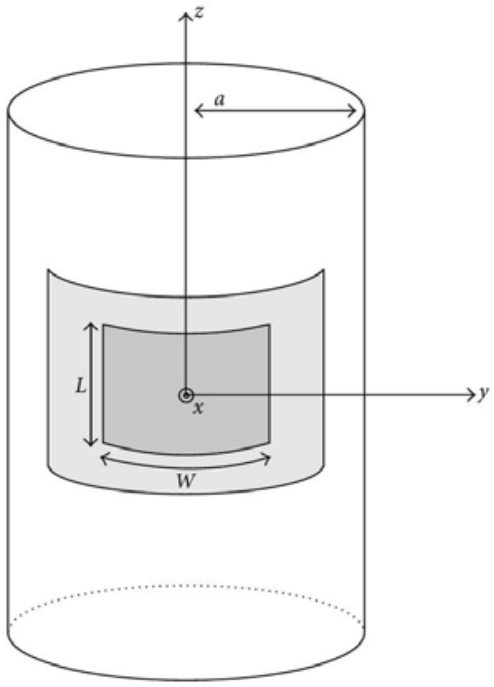


Figure 27 3.3: Single element dimension [3]

The details of the dimensions of the cylinder are given in table below,

Table 1 Table of conformal design dimensions in millimeter

| Type | Material | Dimension | Height | Thickness | Radius |
|---|---|---|---|---|---|
| Patch | Copper | 38.13 x 48.53 | / | / | / |
| Substrate | Rogers RT5880 | / | 535 | 0.8 | 174.61(outer) 173.81(inner) |
| Ground | Copper | / | 535 | / | 173.81 |

### *3.3.1 Rogers RT5880 substrate:*

The fundamental component of every antenna design is the dielectric material chosen. There are numerous substrates available for designing antennas with dielectric constants ranging from 2.2 ≤ε ≤ 12. Those with a dielectric constant near the lower end of the spectrum are preferred for antenna performance because they provide high efficiency, wide bandwidth, and loosely bound radiation fields[3].

In this design, the substrate used is from Rogers which is rogers RT5880. Because RT/duroid 5880 laminates have a low dielectric constant and a low dielectric loss, they are well suitable for large frequency/broadband applications[22]. For more demanding electrical applications, RT/duroid 5880 composites can be covered with rolled copper foil, using electrodeposited copper of ½ to 2 /ft.2 (8 to 70m) or reverse treated EDC on both sides[22].

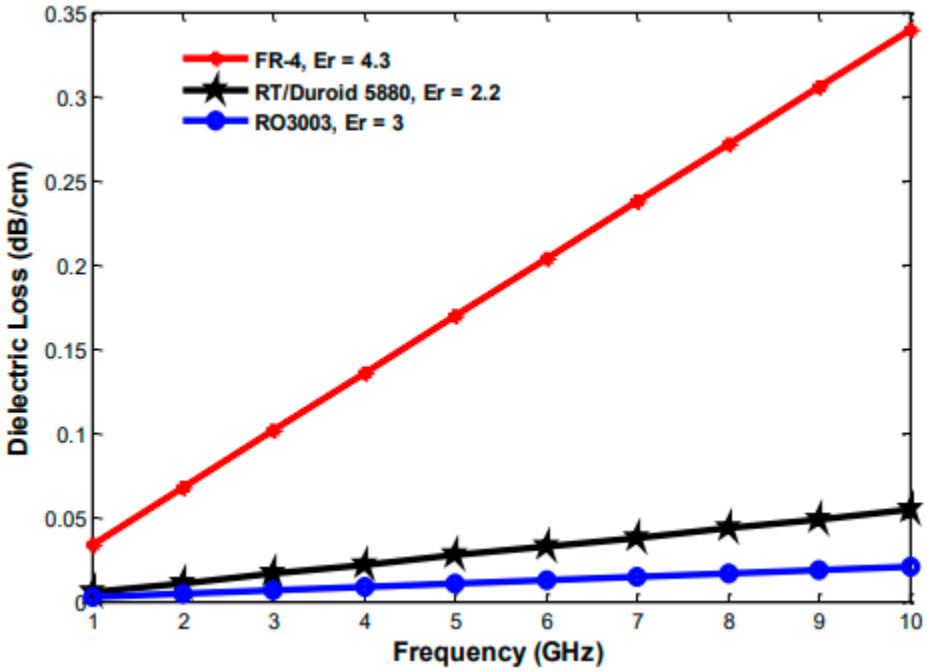


**Figure 28 3.3.1: Dielectric loss versus frequency for different types of dielectric substrate materials [22]**

The primary benefits of RT 5880 include its consistent electrical qualities over a broad frequency range, and suitability for high moisture environments[22].

## *3.4 Simulation Setup and Results:*

After the design of cylinder, discrete port is setup between two points, that are patch and ground passing through substrate. Different position of port is tested until the desired results are obtained. The port excitation type is S-parameter.

The frequency is given in gigahertz (GHz), and the length is given in millimeters. The frequency range is set to between 2Ghz and 2.9Ghz, and the material type is set to standard.

Now, when the discrete port coordinates are "0", "radius", "-lp/2+lp/3" (X,Y,Z) for 1st point and "0", "radius-hs-hs-0.2", "-lp/2+lp/3" for 2nd point,

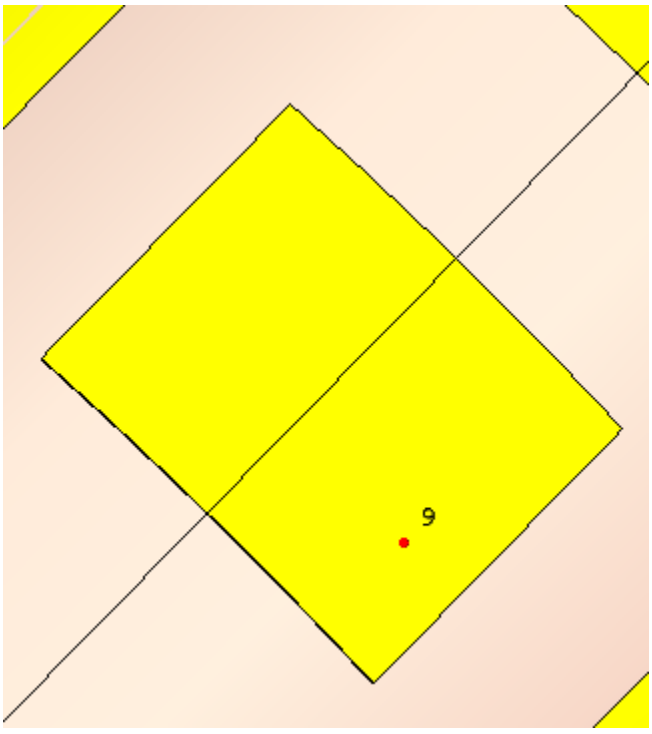


**Figure 29 3.3.2: Discrete port of single element**

The S-parameter is illustrated below,

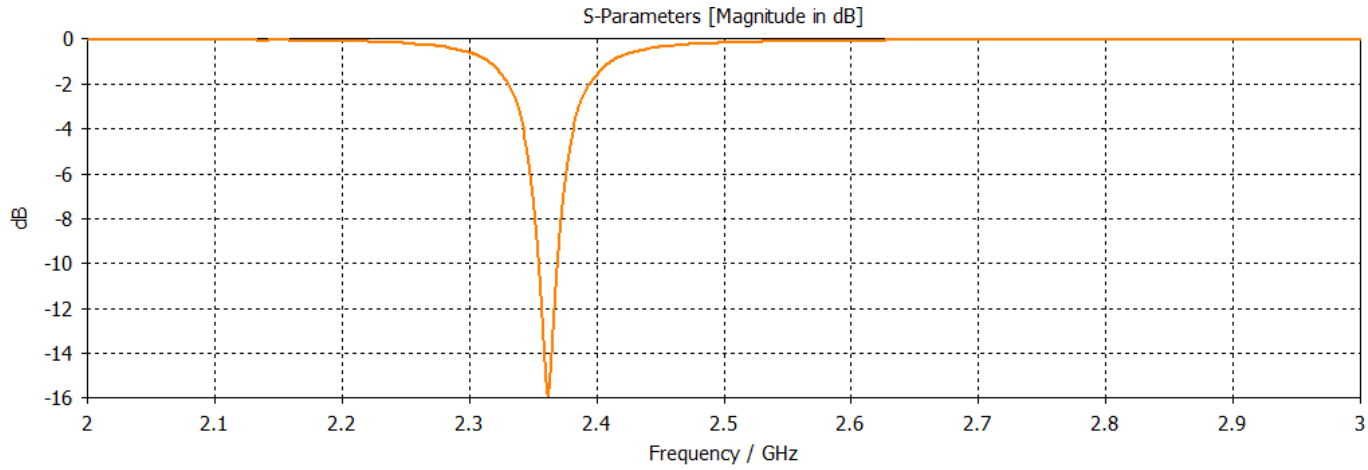


**Figure 30 3.3.2: S-parameter with initial port location**

Then, by changing different location of discrete port where 1st point is "wp/3", "radius-hs", "(-3*lp/2-lp/3)+(2*lp)+(3*spacing)" and 2nd point "wp/3", "radius-3*hs-hs/2", "(-3*lp/2-lp/3)+(2*lp)+(3*spacing)",

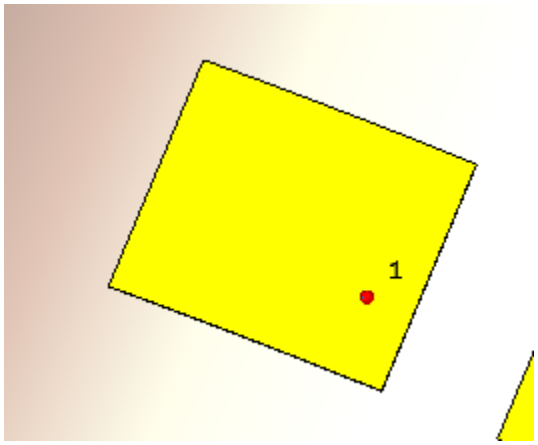


**Figure 31 3.3.2: Repositioned Discrete port location**

As a result, the resulting S-parameter is,

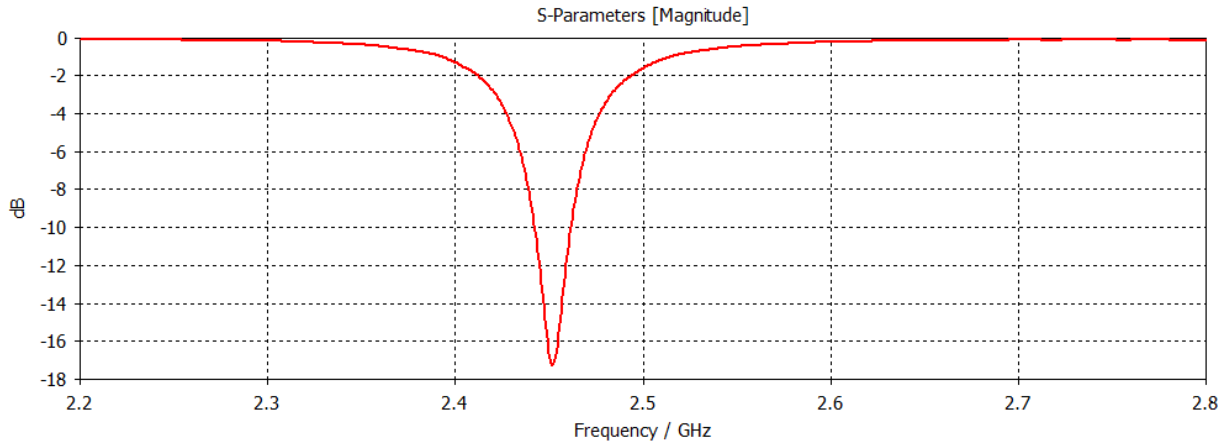


**Figure 32 3.3.2: S-parameter with repositioned port location**

The above graph of S-parameters demonstrates that the patch's resonant frequency point is positioned at 2.45GHz, which is a good matching frequency, and that the patch's center frequency is likewise low.

Further improvement is achieved by using optimization solution with the following configuration,

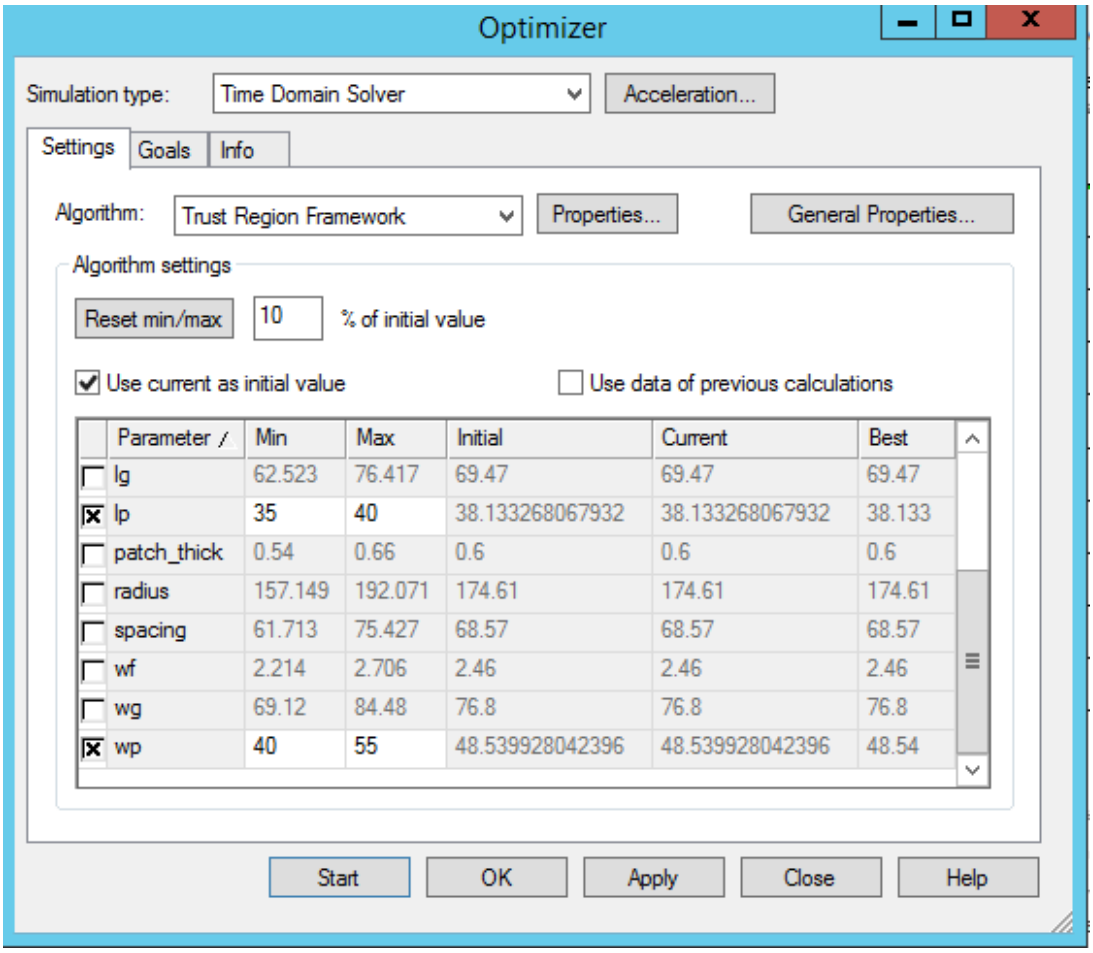


**Figure 33 3.3.2: Optimizer window in CST**

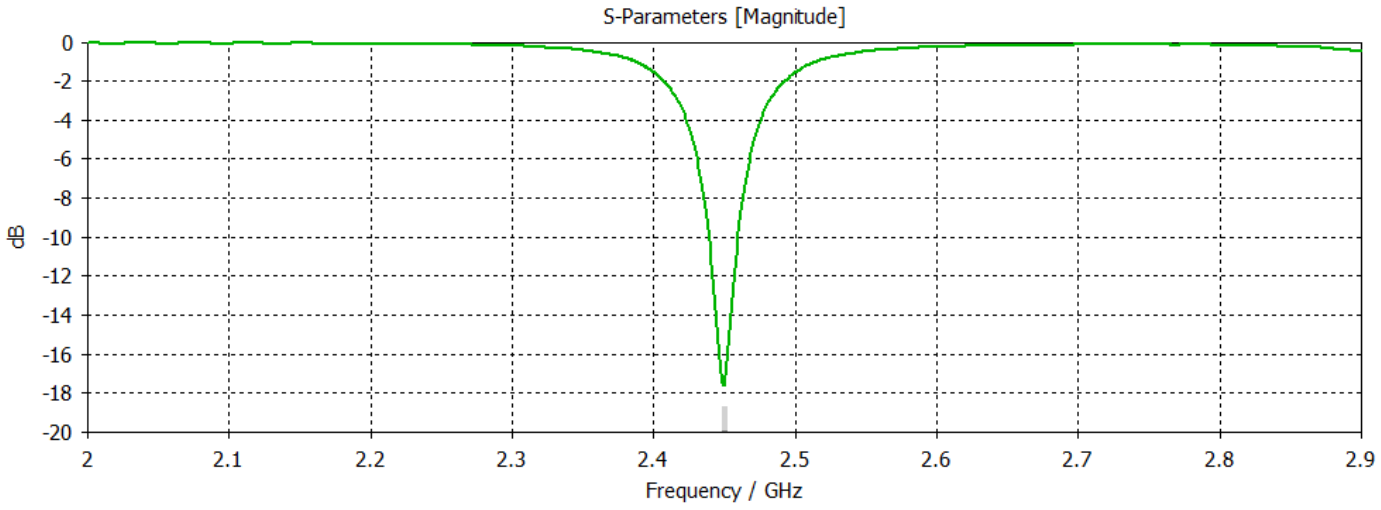


**Figure 34 3.3.2: Resulting S-parameter after optimization**

Each of these modifications was carried out on a single patch until the desired results were reached. After attaining the desired outcome, the port is rotated at an angle of 22.5 degrees using the ‘Rotate' function for the remaining 15 patches in the same circle.

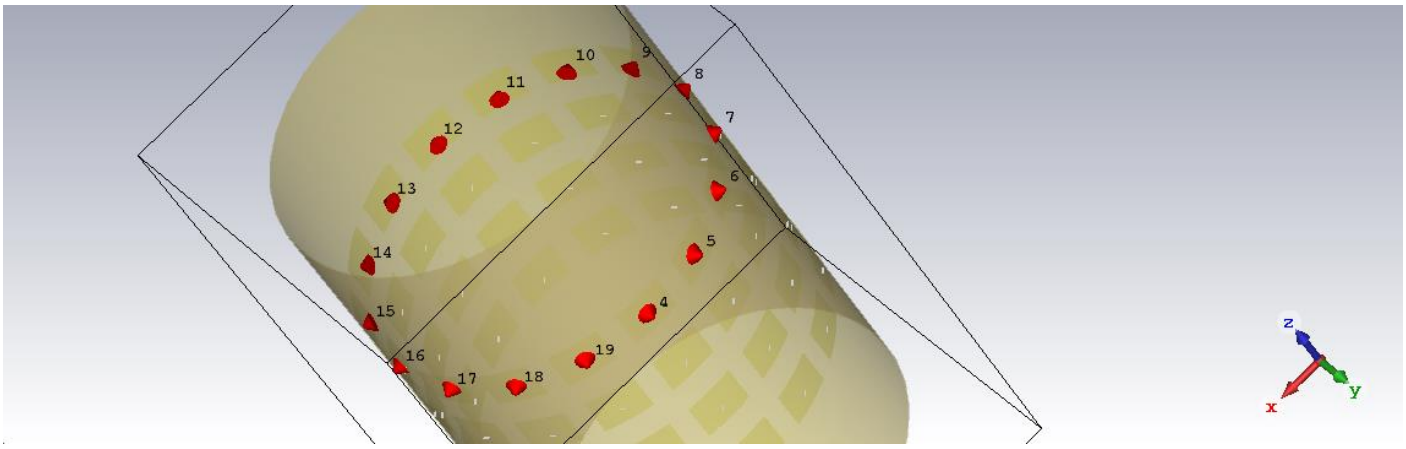


**Figure 35 3.3.2: Discrete Ports using transform function**

Field monitor is setup for Fairfield calculation in 2.45Ghz.

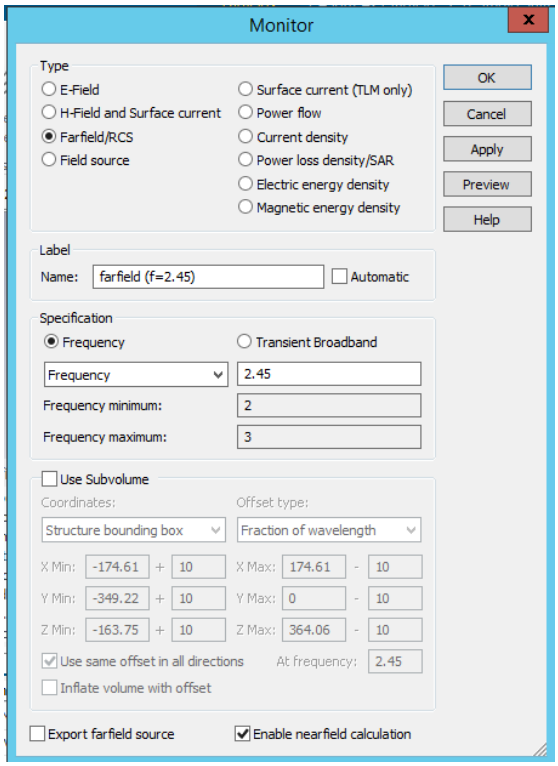


**Figure 36 3.3.2: Field Monitor window in CST**

In far-field, the radiation pattern of an antenna is determined and expressed as a function of the near-field directional coordinates.

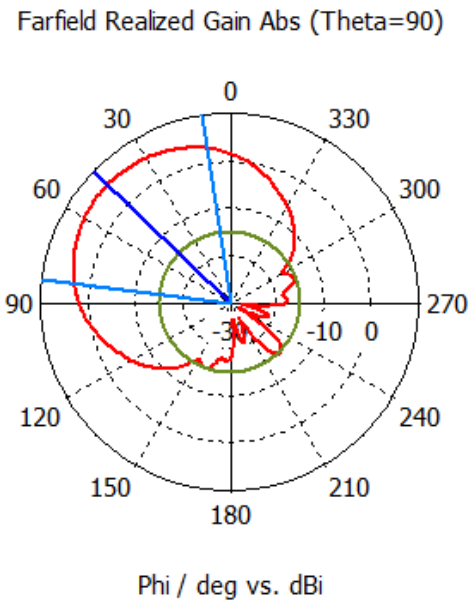


**Figure 37 3.3.2: Polar coordinates representation for equal Amplitude and Phase in XY plane**

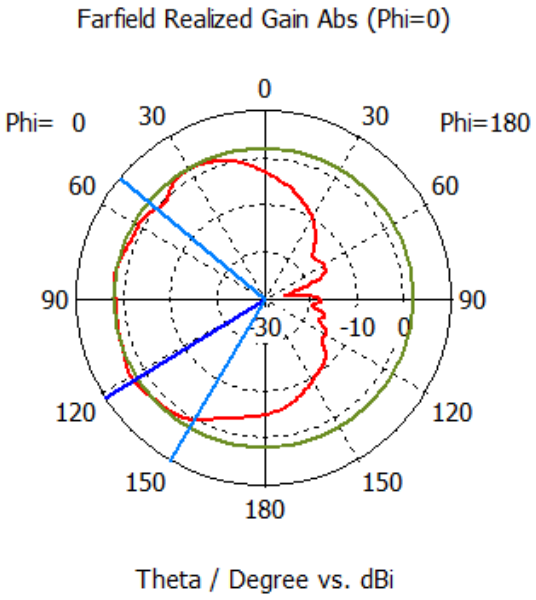


**Figure 38 3.3.2: Polar coordinates representation for equal Amplitude and Phase in XZ plane**

The polar representation of the single element whose S-parameter is depicted in figure 34 is illustrated in the figures above.

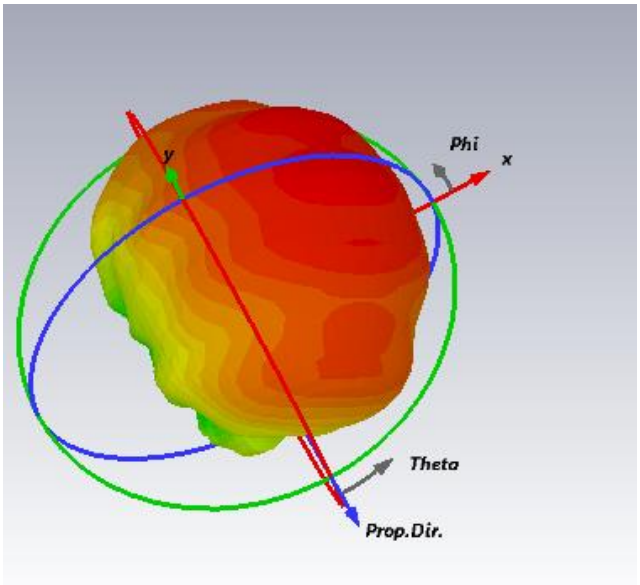


**Figure 39 3.3.2: 3-D representation for equal Amplitude and Phase**

The antenna parameters observed here are the radiation intensity, Gain, directivity and more.

Given that the above findings are from a single element simulation, it is worth noting that the time required to run the simulation is far longer than anticipated. While simulating the full conformal antenna, 4x16 elements, and each element 64 times, it was discovered that it took almost 12 hours to simulate a single patch element.

As a result, the design is adjusted to a 4x5 arrangement in order to attain the desired results within a manageable simulation time.

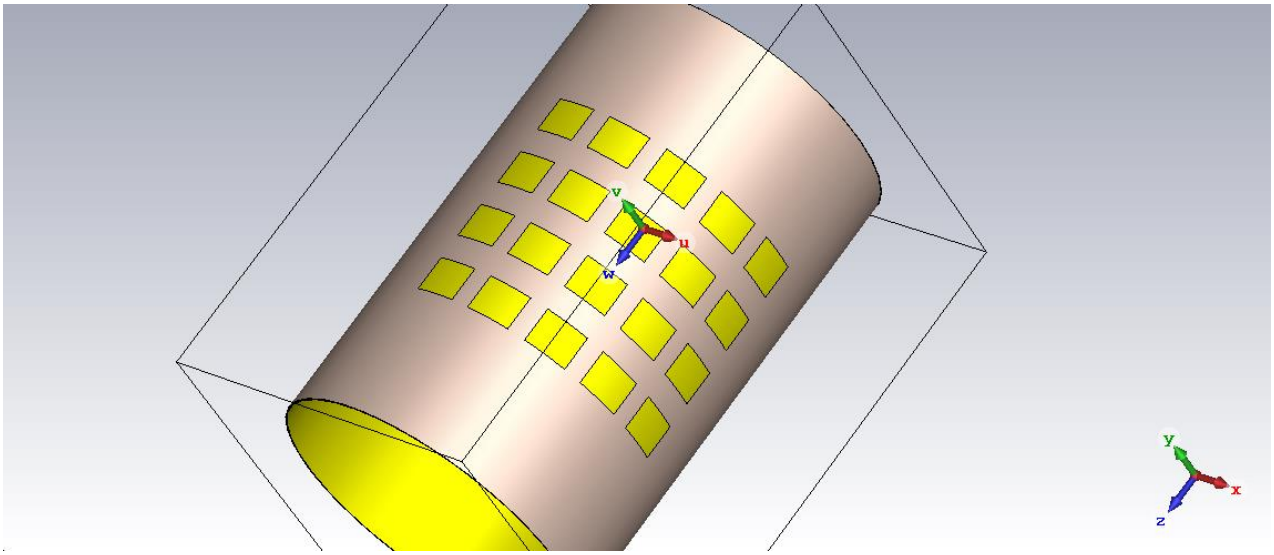


**Figure 40 3.3.2: Conformal antenna of 4x5 configuration**

Discrete ports are used in 3rd column,

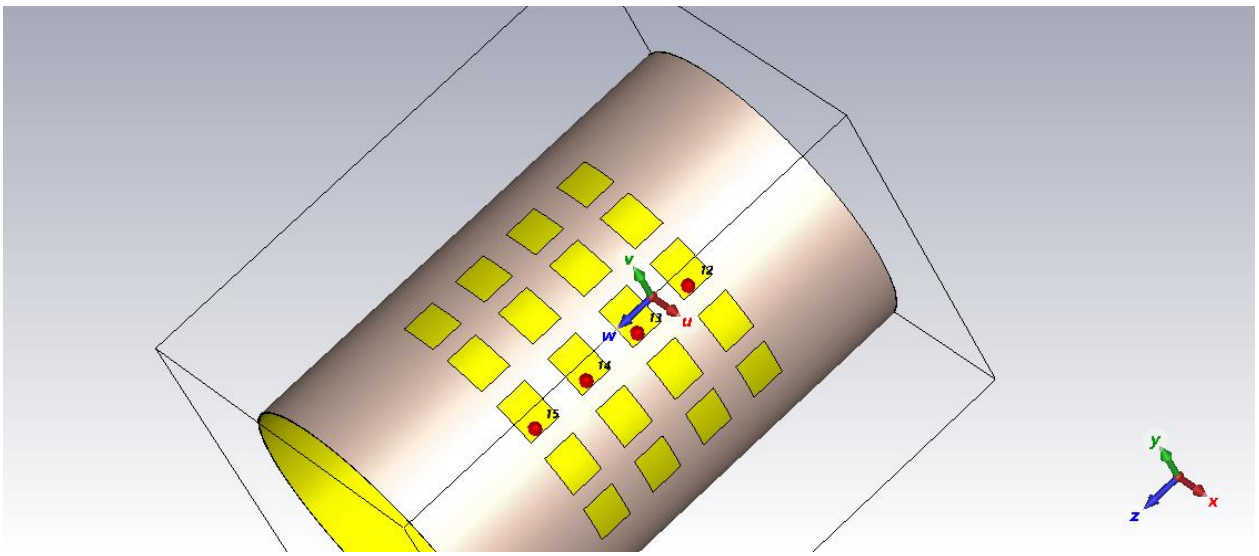


**Figure 41 3.3.2: Discrete ports on center column**

Simulation is then performed on port 12, 13, 14, and 15. Below are the results obtained,

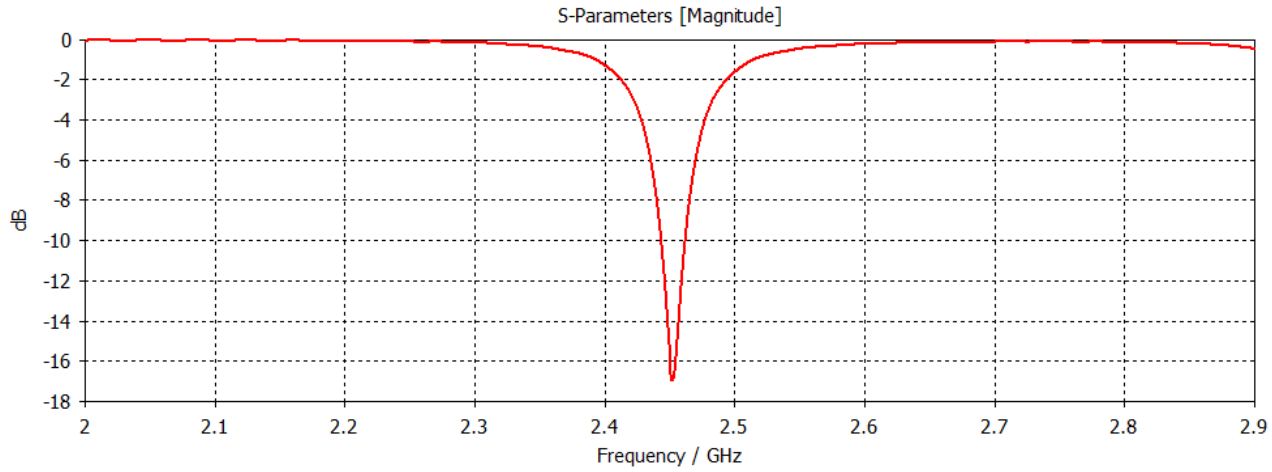


**Figure 42 3.3.2: S-parameter result of port 12**

It can be seen that the minimum return loss of the antenna is -16.9 dB at 2.45 GHz. It has a -10 dB bandwidth of 20MHz. The far-field radiation pattern shows that the directivity and gain of the antenna is 7.80 dBi and 7.02 dBi, respectively. The main lobe magnitude observed 7.45 dBi, main lobe direction is 47°, 3dB angular beamwidth is 68.2° and side lobe level is -20.6 dB.

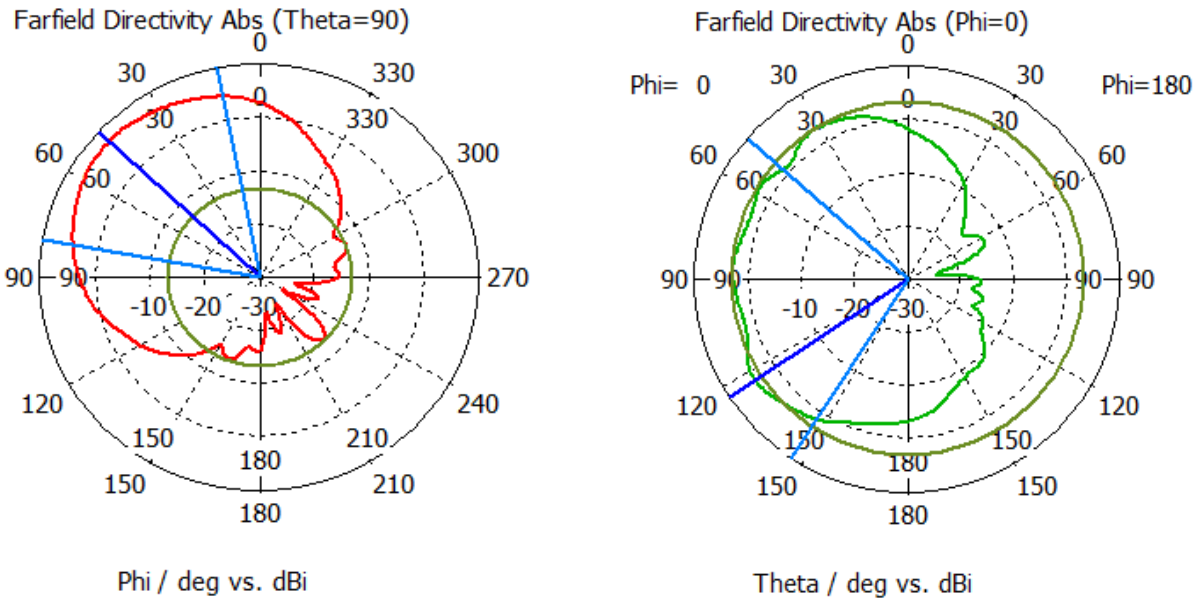


**Figure 43 3.3.2: Polar coordinates representation of equal amplitude and phase of port 12**

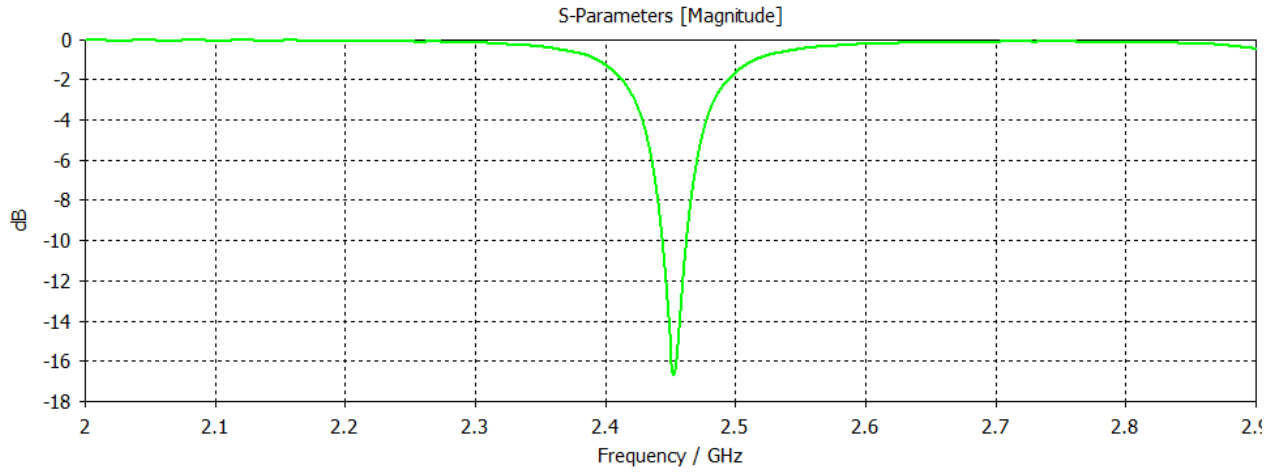


**Figure 44 3.3.2: S-parameter result of port 13**

It can be seen that the minimum return loss of the antenna is -17.04 dB at 2.45 GHz. It has a -10 dB bandwidth of 20MHz. The far-field radiation pattern shows that the directivity and gain of the antenna is 7.40 dBi and 6.713 dBi, respectively. The main lobe magnitude observed 5.93 dBi, main lobe direction is 47°, 3dB angular beamwidth is 69.5° and side lobe level is -31.6 dB.

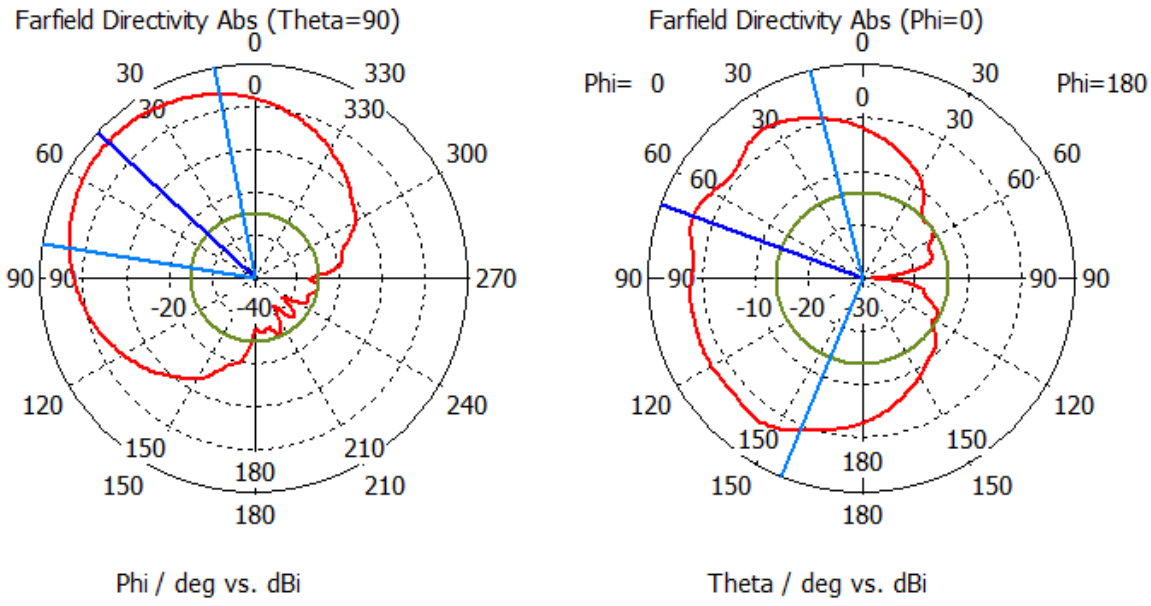


**Figure 45 3.3.2: Polar coordinates representation of equal amplitude and phase of port 13**

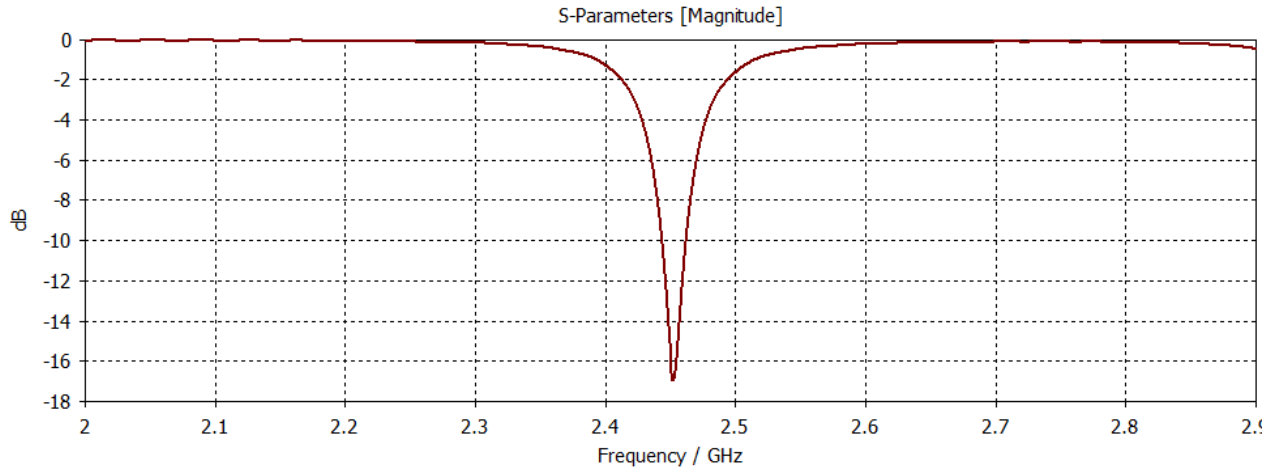


**Figure 46 3.3.2: S-parameter result of port 14**

It can be seen that the minimum return loss of the antenna is -16.98 dB at 2.45 GHz. It has a -10 dB bandwidth of 190MHz. The far-field radiation pattern shows that the directivity and gain of the antenna is 7.441 dBi and 6.661 dBi, respectively. The main lobe magnitude observed 6.61 dBi, main lobe direction is 47°, 3dB angular beamwidth is 71.6° and side lobe level is -28.6 dB.

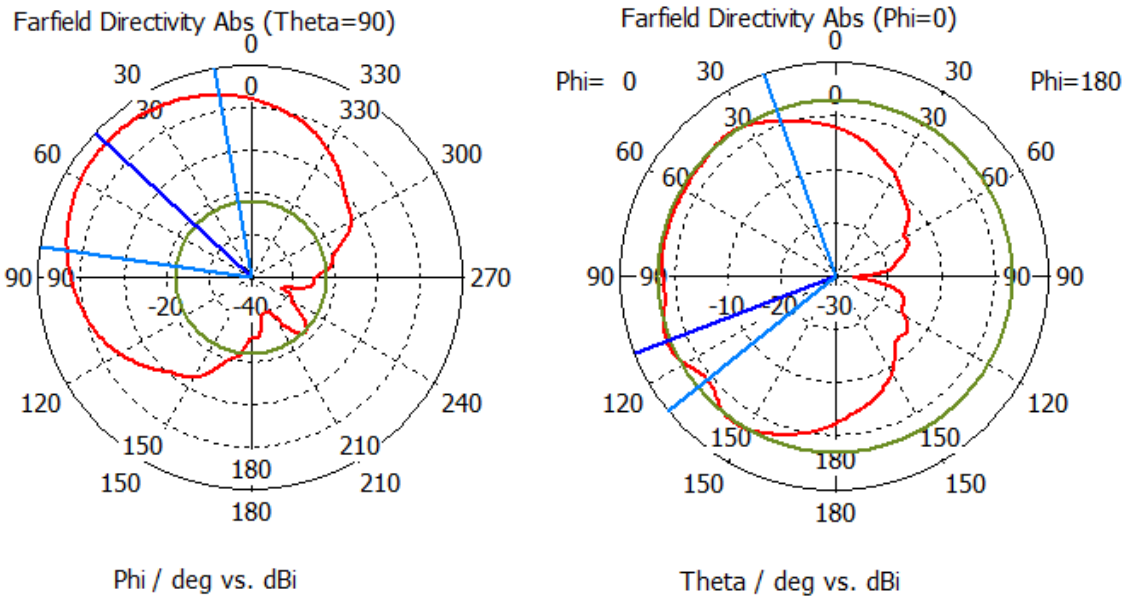


**Figure 47 3.3.2: Polar coordinates representation of equal amplitude and phase of port 14**

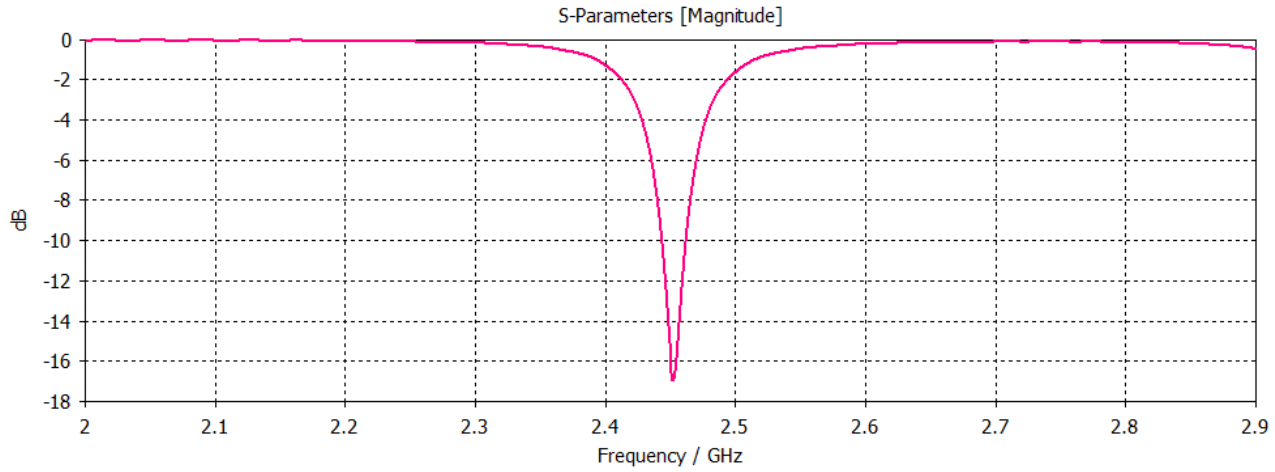


**Figure 48 3.3.2: S-parameter result of port 15**

It can be seen that the minimum return loss of the antenna is -17.19 dB at 2.45 GHz. It has a -10 dB bandwidth of 210MHz. The far-field radiation pattern shows that the directivity and gain of the antenna is 7.760 dBi and 6.981 dBi, respectively. The main lobe magnitude observed 6.72 dBi, main lobe direction is 47°, 3dB angular beamwidth is 66.4° and side lobe level is -19.7 dB.

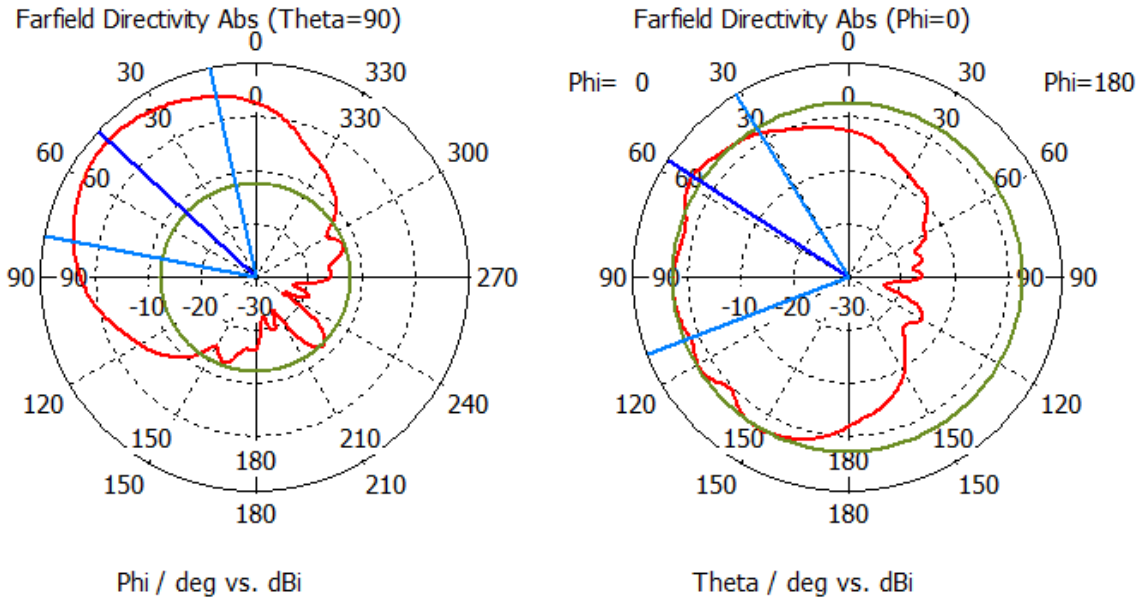


**Figure 49 3.3.2: Polar coordinates representation of equal amplitude and phase of port 15**

Due to the fact that each element of the conformal antenna has a separate discrete port feed, CST will simulate each port in a queue. Other ports will then automatically adjust their absorbency to comply. As a result, when the simulation is complete, the active radiation pattern for each element is obtained.

As we already know the radiation pattern for each element, the **'Combine Result'** option in CST post-processing is employed to generate the pattern synthesis.

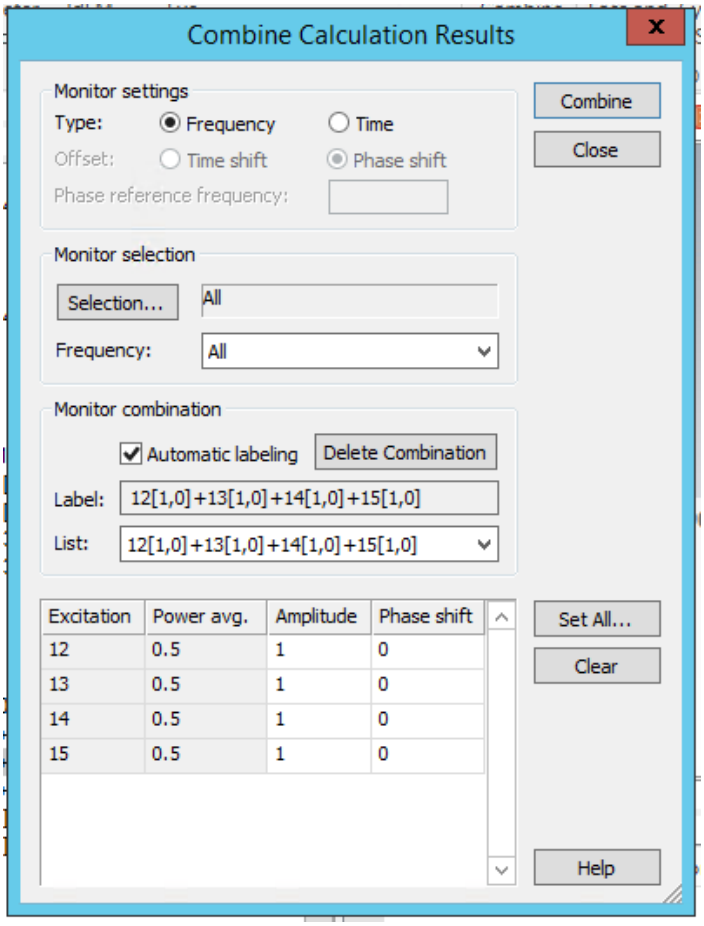


The amplitude and phase parameters are listed below, followed by their radiation pattern,

### *3.4.1 When having same Amplitude and Phase shift:*

**Table 2 Post processing parameters of same amplitude and Phase shift**

| Excitation | Power avg. | Amplitude | Phase Shift |
|---|---|---|---|
| 12 | 0.5 | 1 | 0 |
| 13 | 0.5 | 1 | 0 |
| 14 | 0.5 | 1 | 0 |
| 15 | 0.5 | 1 | 0 |

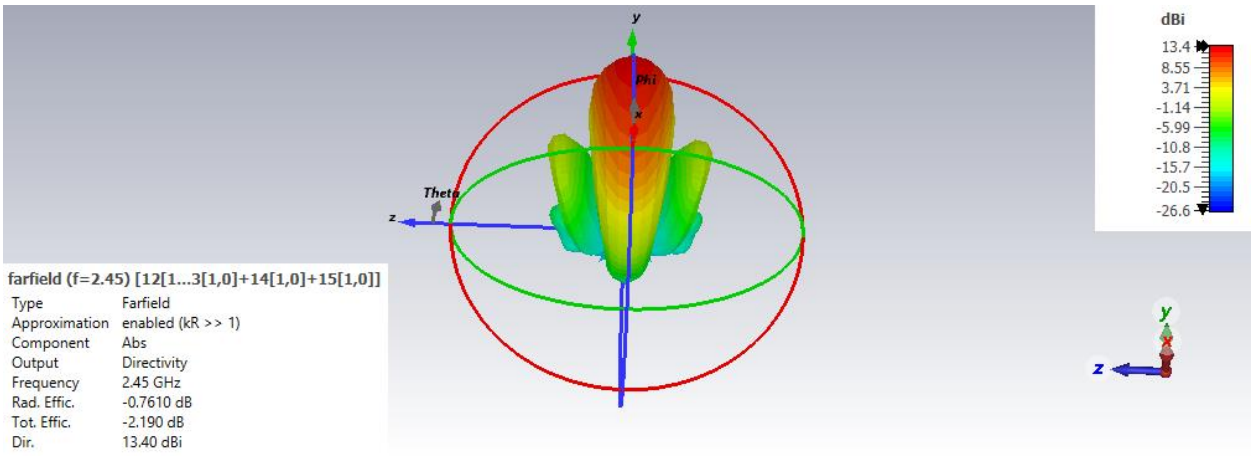


**Figure 50 3.4: 3-D representation of Farfield with same amplitude and phase shift**

The 3D radiation pattern can be observed in figure 50 in which it can be seen that we have narrower beamwidth of far field performance having directivity of 13.40dBi and gain of 12.64dBi. The element radiation pattern is observed when there is no changes were made to its amplitude or phase.

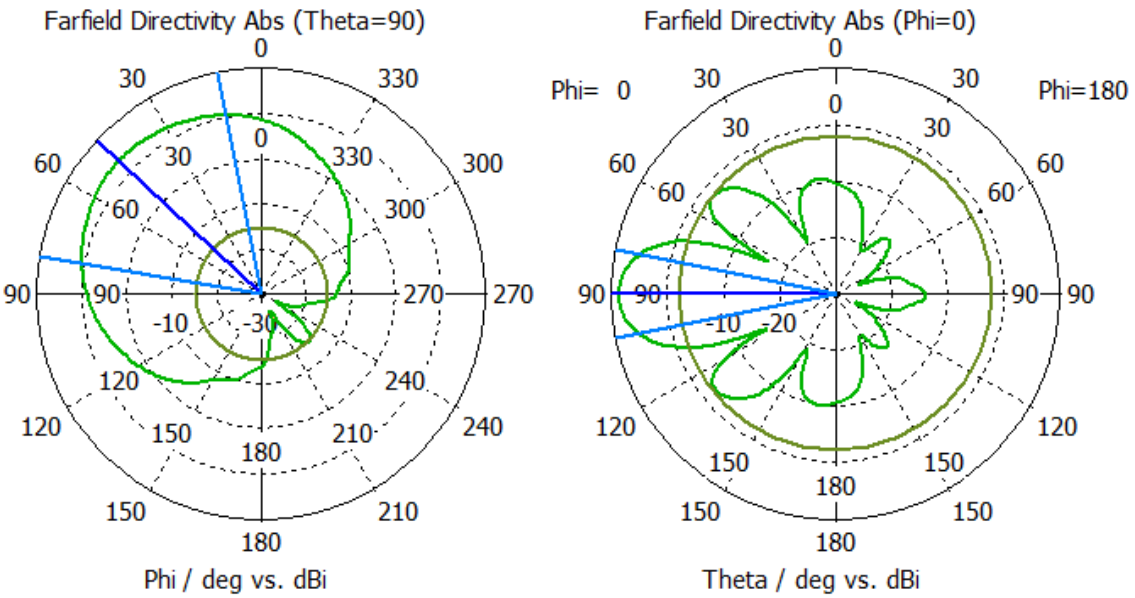


**Figure 51 3.4: Polar coordinate representation of same amplitude and phase shift**

As illustrated in figure 51, the primary lobe direction is parallel to the axis plane simply due to the identical phase shift. The primary lobe has a magnitude of 8.64 dBi and a direction of 90°.

### *3.4.2 When having same Amplitude but positive Phase shift:*

**Table 3 Post processing parameters of same amplitude and different Phase shift**

| Excitation | Power avg. | Amplitude | Phase Shift |
|---|---|---|---|
| 12 | 0.5 | 1 | 60 |
| 13 | 0.5 | 1 | 120 |
| 14 | 0.5 | 1 | 180 |
| 15 | 0.5 | 1 | 240 |

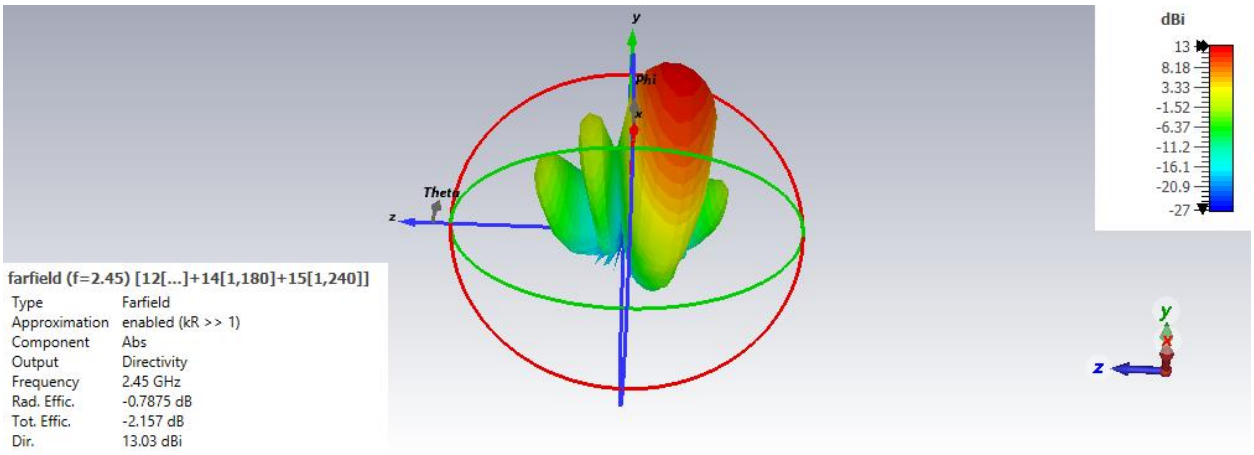


**Figure 52 3.4: 3-D representation of Farfield with same amplitude and positive phase shift**

The 3D radiation pattern can be observed in figure 52 in which it can be seen that we have narrower beamwidth of far field performance having directivity of 13.03dBi and gain of 12.24dBi.

The radiation pattern in observed with the beam of antenna is steered with positive phase shift of 60$^{o}$ in each element. Therefore, there is change observed in the resulting beam compared to case 1 with slight drop in gain value.

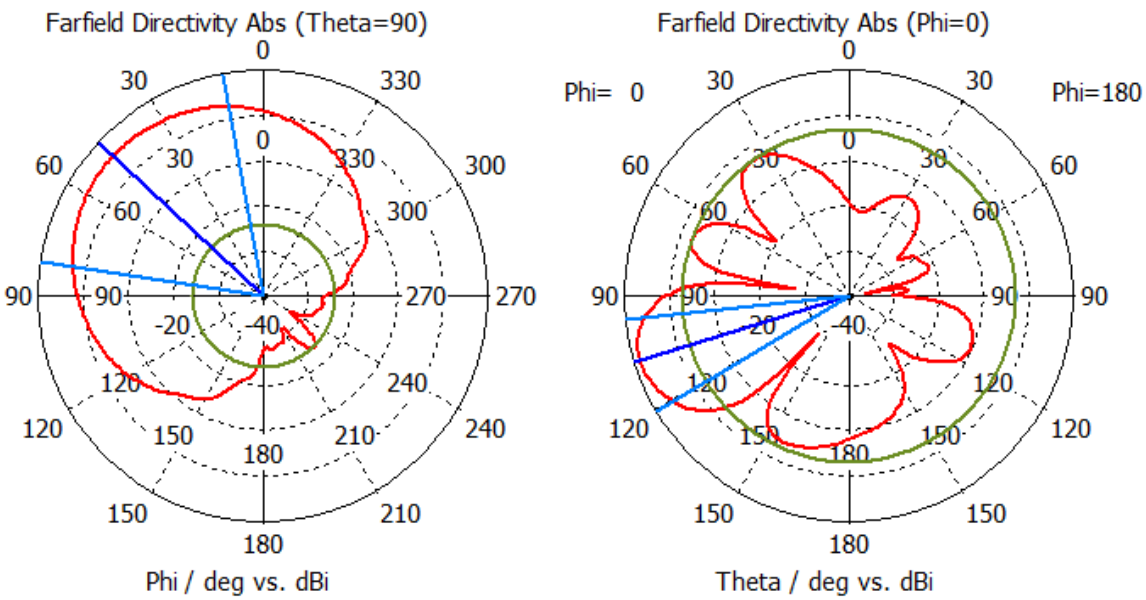


**Figure 53 3.4: Polar coordinate representation of same amplitude and positive phase shift**

As illustrated in Figure 53, when the phase of the elements is changed to positive degrees, the orientation of the main lobe likewise changes from 90 to 107°, a change of 17°. This also leads in a shift in the magnitude of the major lobe, which is now 8.57dBi.

### *3.4.3 When having same Amplitude and negative Phase shift:*

**Table 4 Post processing parameters of same amplitude and negative Phase shift**

| Excitation | Power avg. | Amplitude | Phase Shift |
|---|---|---|---|
| 12 | 0.5 | 1 | -60 |
| 13 | 0.5 | 1 | -120 |
| 14 | 0.5 | 1 | -180 |
| 15 | 0.5 | 1 | -240 |

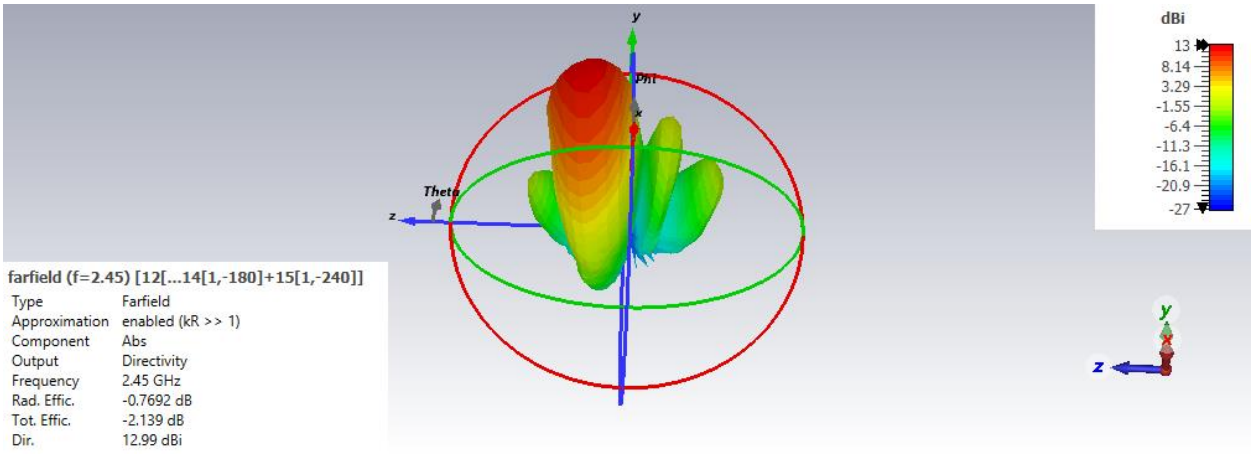


**Figure 54 3.4: 3-D representation of Farfield with same amplitude and negative phase shift**

The 3D radiation pattern can be observed in figure 54 in which it can be seen that we have narrower beamwidth of far field performance having directivity of 12.99dBi and gain of 12.22dBi.

The radiation pattern in observed with the beam of antenna is steered with negative phase shift of $60^{o}$ in each element but with similar amplitude. Direction of the resulting beam changes in clockwise direction with shift of $18^{o}$.

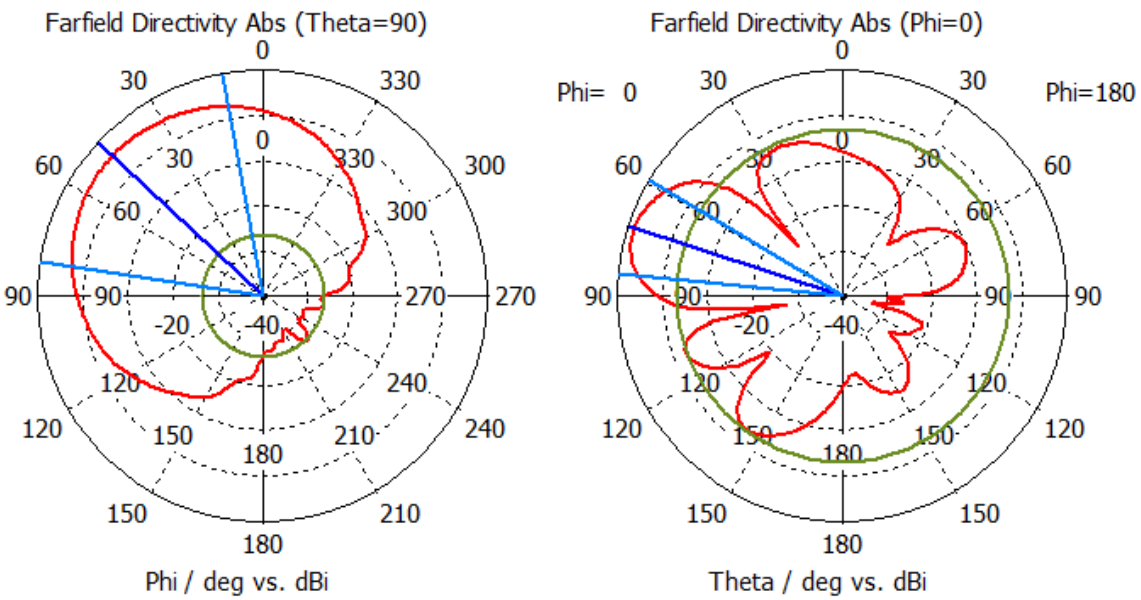


**Figure 55 3.4: Polar coordinate representation of same amplitude and negative phase shift**

As illustrated in Figure 55, the resulting pattern occurs when the phase shift is performed in the negative direction. The direction of the main lobe has been changed to 72°, and the magnitude of the main lobe has been increased to 8.57dBi.

### *3.4.4 When having different amplitude and positive Phase shift:*

**Table 5 Post processing parameters of both different amplitude and Phase shift**

| Excitation | Power avg. | Amplitude | Phase Shift |
|---|---|---|---|
| 12 | 0.5 | 1 | 0 |
| 13 | 1.125 | 1.5 | 45 |
| 14 | 2 | 2 | 90 |
| 15 | 3.125 | 2.5 | 135 |

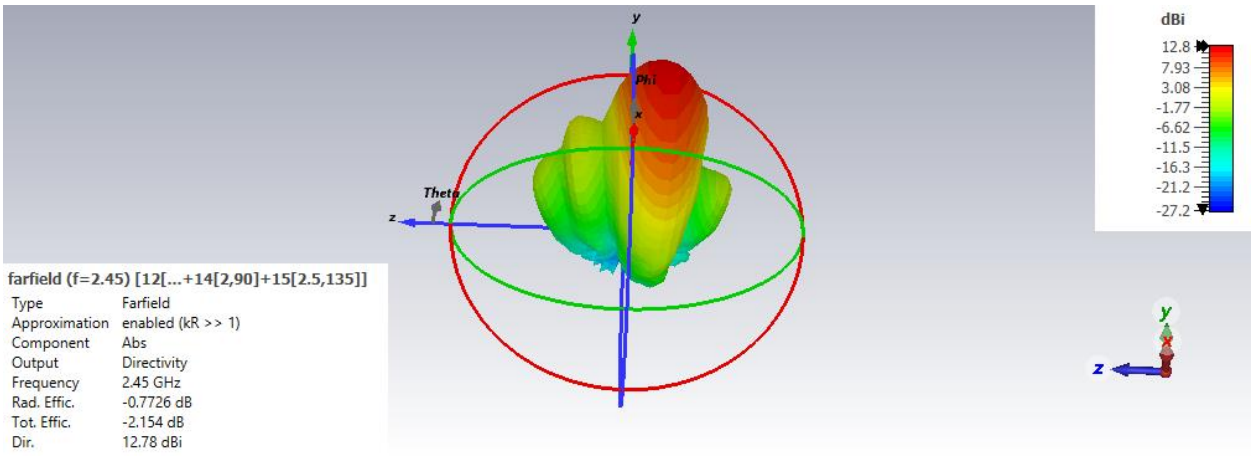


**Figure 56 3.4: 3-D representation of Farfield with different amplitude and positive phase shift**

The 3D radiation pattern can be observed in figure 56 in which it can be seen that we have narrower beamwidth of far field performance having directivity of 12.78dBi and gain of 12.00dBi.

The radiation pattern in observed with there is positive phase shift of 45$^{o}$ and change in amplitude of each element. It is observed that there is slight drop in gain value and increase side lobes.

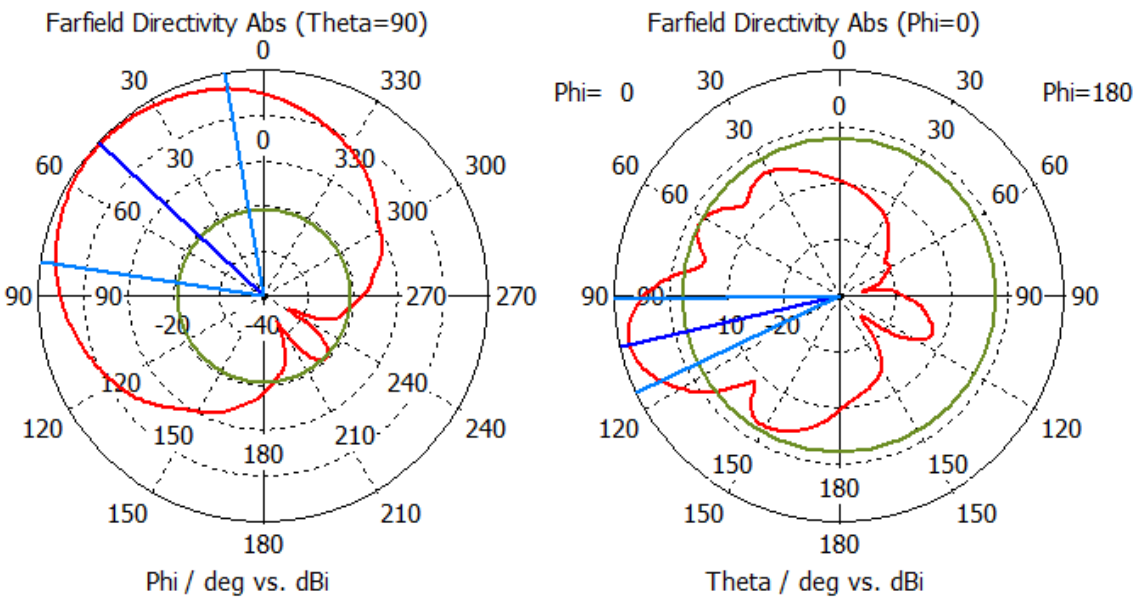


**Figure 57 3.4: Polar coordinate representation of different amplitude and positive phase shift**

The results of the radiation pattern when the amplitude and phase shift of the elements are changed are depicted in Figure 57. The resulting major lobe is angled at 103°, with a magnitude of 8.17dBi.

### *3.4.5 When having different amplitude and negative Phase shift:*

**Table 6 Post processing parameters of different amplitude and negative Phase shift**

| Excitation | Power avg. | Amplitude | Phase Shift |
|---|---|---|---|
| 12 | 0.5 | 1 | 0 |
| 13 | 1.125 | 1.5 | -45 |
| 14 | 2 | 2 | -90 |
| 15 | 3.125 | 2.5 | -135 |

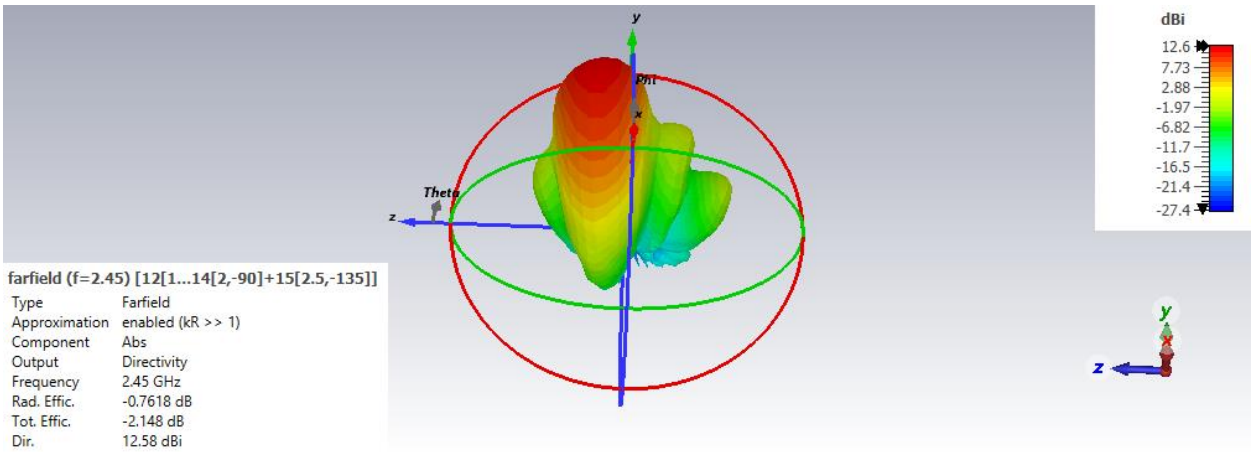


**Figure 58 3.4: 3-D representation of Farfield with different amplitude and negative phase shift**

The 3D radiation pattern can be observed in figure 58 in which it can be seen that we have narrower beamwidth of far field performance having directivity of 12.58dBi and gain of 11.82dBi.

The radiation pattern in observed with there is negative phase shift of 45° and change in amplitude of each element is same as case 4.

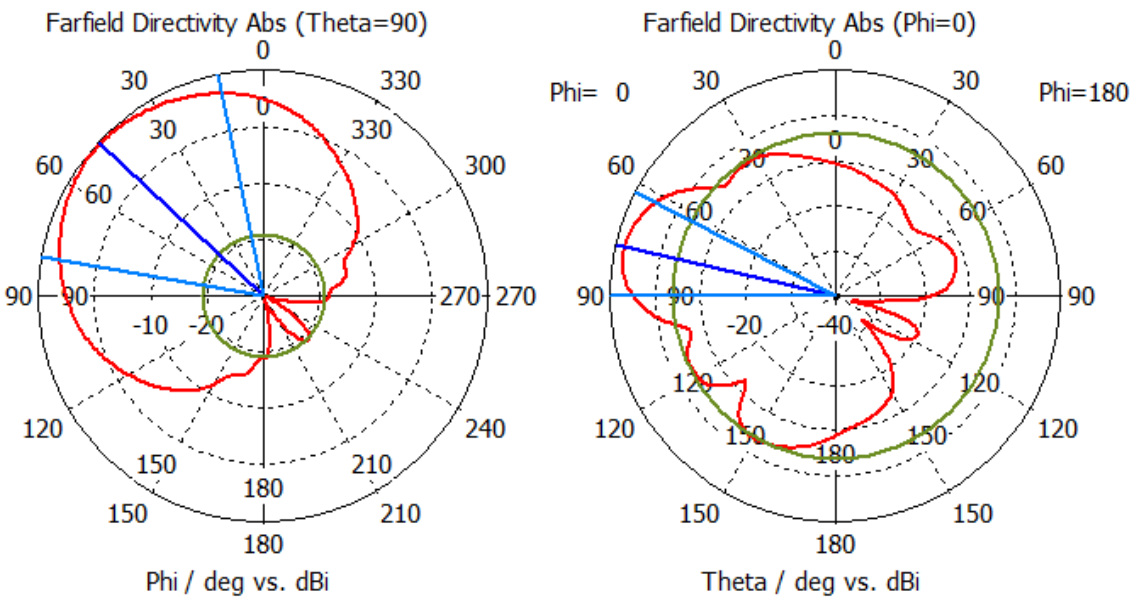


**Figure 59 3.4: Polar coordinate representation of different amplitude and negative phase shift**

The radiation illustration shown in Figure 59 occurs when the amplitude changes with negative phase. The primary lobe has a magnitude of 7.99dBi and a direction of 77°.

# Chapter 4: Conclusion

Numerous technical and non-technical components of this thesis can be evaluated. From a technical perspective, it is critical to consider crucial factors such as radiation pattern, gain, phase shift, and VSWR while designing the antenna. These are crucial components for both conventional and conformal antennas, and some of them, such as gain and radiation pattern, are application dependent.

The conformal array antenna on the cylinder's surface is presented in this thesis. Time-domain solvers, optimization, as well as other similar techniques are applied during the design process. Additionally, the antenna array's beam scanning performance is also performed.

It is worth mentioning that the properties of an antenna vary according on its physical parameters. For instance, the width of the dielectric and even the ground plane alters the antenna's bandwidth due to a phenomenon called fringing. Additionally, the gain and directivity of the antenna are also related to ground plane. The radiation pattern varies according to the antenna's environment. Similarly, dielectric constant has an effect on the gain, reflection coefficient, and bandwidth characteristics. By altering the antenna dielectric, we may also alter the antenna's radiated power and return loss.

Once antenna is designed, the simulation is performed using CST microwave studio software. At first, each antenna element's radiation pattern is calculated by solving it separately. Then optimization is performed for desired 2.45Ghz frequency using both parameters sweep and post processing optimization. Then the simulation of all patch elements is performed, and the resulting Farfield radiation patterns are then discussed with s11 parameters.

Beam scanning is performed by using the post processing method in CST, in which different phase and amplitude parameters are assigned to the conformal antenna and there radiation pattern is studied.

The proposed antenna design provides the gain of 8.64 dBi when amplitude is unity and phase shift is 0. The gain of an antenna changes to 8.57dBi and the direction of antenna

changes when there is positive phase shift, and it becomes 8.17dBi when there is change in both amplitude and phase shift.

For future work, the proposed design can be further improved in terms of gain, radiation pattern and beamforming scanning capabilities. It can be achieved by increasing the patch elements on the conformal antenna. However, a trade-off analysis between patch elements parameters and port feeding techniques will be required.

# Bibliography


[1] “Antenna Gain - an overview | ScienceDirect Topics.” https://www.sciencedirect.com/topics/engineering/antenna-gain (accessed Jun. 11, 2021).

[2] “(PDF) Optimization of Digital Beamforming for Smart Antennas.” https://www.researchgate.net/publication/312583657_Optimization_of_Digital_Beamforming_for_Smart_Antennas (accessed Jun. 11, 2021).

[3] “Antenna Theory Analysis and Design By Constantine A Balanis- By EasyEngineering.net”.

[4] “(PDF) Reconfigurable Phased Array Patch Antenna for Ku-Band Satellite Communication Systems نطاق على الصناعية االقمار اتصاالت ألنظمة الرقيقة الشرائح هوائيات مصفوفة تصميم Ku Moahmmed Awny Matar.” https://www.researchgate.net/publication/326677601_Reconfigurable_Phased_Array_Patch_Antenna_for_Ku-Band_Satellite_Communication_Systems_ntaq_ly_alsnayt_aalqmar_atsaalt_alnzmt_alrqyqt_alshrayh_hwayyat_msfwft_tsmym_Ku_Moahmmed_Awny_Matar/figur.es?lo=1 (accessed Jun. 11, 2021)

[5] “What are Near Field and Far Field Regions of an Antenna? - everything RF.” https://www.everythingrf.com/community/what-are-near-field-and-far-field-regions-of-an-antenna (accessed Jun. 11, 2021).

[6] “RF Components & Test Equipment - everything RF.” https://www.everythingrf.com/ (accessed Jun. 11, 2021).

[7] D. K. Cheng, *Field and Wave Electromagnetics - Solution Manual*, vol. 28, no. 2. 1989.

[8] D. G. Riviello and R. Garello, “Implementation of 5G beamforming techniques on cylindrical arrays,” in *Proceedings of the 2019 9th IEEE-APS Topical Conference on Antennas and Propagation in Wireless Communications, APWC 2019*, Sep. 2019, pp. 413–418. doi: 10.1109/APWC.2019.8870441.

[9] “What is 5G beamforming, beam steering and beam switching with massive MIMO.” https://www.metaswitch.com/knowledge-center/reference/what-is-beamforming-beam-steering-and-beam-switching-with-massive-mimo (accessed Jun. 13, 2021).

[10] “GRUPPO TELECOM ITALIA 5G workshop Workshop: Evolution from 4G to 5G.”

[11] A. Singh, A. Kumar, A. Ranjan, A. Kumar, and A. Kumar, “Beam Steering in Antenna.”

[12] S. Ghosh and D. Sen, “An Inclusive Survey on Array Antenna Design for Millimeter-Wave Communications,” *IEEE Access*, vol. 7, pp. 83137–83161, 2019, doi: 10.1109/ACCESS.2019.2924805.

[13] D. G. Riviello and D. G. Riviello, “Planar and circular array processing and beamforming techniques for 5G cellular systems,” 2019.

[14] Y. B. Nechaev, I. W. Peshkov, and N. A. Fortunova, “Cylindrical antenna array development and measurments for DOA-estimation applications,” in *2017 11th International Conference on Antenna Theory and Techniques, ICATT 2017*, Jul. 2017, pp. 155–158. doi: 10.1109/ICATT.2017.7972608.

[15] H. Rammal, C. Olleik, K. Sabbah, M. Rammal, and P. Vaudon, “Synthesis of Phased Cylindrical Arc Antenna Arrays,” *International Journal of Antennas and Propagation*, vol. 2009, pp. 1–5, 2009, doi: 10.1155/2009/691625.

[16] L. Josefsson and P. Persson, .“1 THE DEFINITION OF A CONFORMAL ANTENNA,” 2006.

[17] R. E. Munson, “Conformal Microstrip Atennas and Microstrip Phased Arrays,” *IEEE Transactions on Antennas and Propagation*, vol. AP-22, no. 1, 1974, doi: 10.1109/TAP.1974.1140723.

[18] P. Yang, F. Yang, Z. P. Nie, B. Li, and X. F. Tang, “Robust adaptive beamformer using interpolation technique for conformal antenna array,” *Progress In Electromagnetics Research B*, no. 23, pp. 215–228, 2010, doi: 10.2528/PIERB10061504.

[19] “CST Studio Suite 3D EM simulation and analysis software.” https://www.3ds.com/products-services/simulia/products/cst-studio-suite/ (accessed Jun. 16, 2021).

[20] L. Josefsson and P. Persson, “Conformal Array Antenna Theory and Design {IEEE Press Series On Electromagnetic Wave Theory}.”

[21] K. S. Beenamole, C. A. Sreejith, and G. Shankar, “Studies on conformal antenna arrays placed on cylindrical curved surfaces,” in *Proceedings of the 2016 International Symposium on Antennas and Propagation, APSYM 2016*, Jul. 2016, pp. 75–77. doi: 10.1109/APSYM.2016.7929157.

[22] “RT/duroid ® 5870 /5880 High Frequency Laminates Some Typical Applications: • Commercial Airline Broadband Antennas • Microstrip and Stripline Circuits • Millimeter Wave Applications • Military Radar Systems • Missile Guidance Systems • Point to Point Digital Radio Antennas,” 2017.